Cortical surfaces mediate the relationship between polygenic scores for intelligence and general intelligence

Tristram A. Lett[1#*], Bob O. Vogel[1#], Stephan Ripke[1,2,3], Carolin Wackerhagen[1], Susanne Erk[1], Swapnil Awasthi[1,3], Vassily Trubetskoy[1,3], Eva J. Brandl[1], Sebastian Mohnke[1], Ilya M. Veer[1], Markus M. Nöthen[4,5], Marcella Rietschel[6], Franziska Degenhardt[4,5], Nina Romanczuk-Seiferth[1], Stephanie H. Witt[6], Tobias Banaschewski[7], Arun L.W. Bokde[8], Christian Büchel[9], Erin B. Quinlan[10], Sylvane Desrivières[10], Herta Flor[11,12], Vincent Frouin[13], Hugh Garavan[14], Penny Gowland[15], Bernd Ittermann[16], Jean-Luc Martinot[17], Marie-Laure Paillère Martinot[18], Frauke Nees[7,11], Dimitri Papadopoulos Orfanos[13], Tomáš Paus[19], Luise Poustka[20], Juliane H. Fröhner[21], Michael N. Smolka[21], Robert Whelan[22], Gunter Schumann[10] and the IMAGEN consortium, Heike Tost[6], Andreas Meyer-Lindenberg[6], Andreas Heinz[1], Henrik Walter[1*]

Shared first authorship

* Corresponding authors:

Address: Division of Mind and Brain Research, Department of Psychiatry and Psychotherapy CCM, Charité - Universitätsmedizin Berlin; Charitéplatz 1, D-10117 Berlin, Germany.

Email: tristram.lett@charite.de; henrik.walter@charite.de

Telephone: +49 30 450 517 141

Running title: Brain mediators of polygenic score for intelligence

Keywords: Intelligence, Genetics, Mediation, Cortical thickness, Surface area

Department of Psychiatry and Psychotherapy CCM, Charité - Universitätsmedizin Berlin, corporate member of Freie Universität Berlin, Humboldt-Universität zu Berlin, and Berlin Institute of Health, Berlin, Germany

2 Analytic and Translational Genetics Unit, Massachusetts General Hospital, Boston MA 02114, USA
3 Stanley Center for Psychiatric Research, Broad Institute of MIT and Harvard, Cambridge MA 02142, USA
4 Department of Genomics, Life & Brain Center, University of Bonn, Sigmund-Freud-Str. 25, 53127 Bonn, Germany
[5] Institute of Human Genetics, University of Bonn, Sigmund-Freud-Str. 25, 53127 Bonn, Germany
[6] Central Institute of Mental Health, University of Heidelberg, Square J5, 68159 Mannheim, Germany
[7] Department of Child and Adolescent Psychiatry and Psychotherapy, Central Institute of Mental Health, University of Heidelberg, Square J5, 68159 Mannheim, Germany
[8] Discipline of Psychiatry, School of Medicine and Trinity College Institute of Neuroscience, Trinity College Dublin
[9] University Medical Centre Hamburg-Eppendorf, House W34, 3.OG, Martinistr. 52, 20246, Hamburg, Germany
[10] Medical Research Council – Social, Genetic and Developmental Psychiatry Centre, Institute of Psychiatry, Psychology & Neuroscience, King's College London, United Kingdom
[11] Department of Cognitive and Clinical Neuroscience, Central Institute of Mental Health, Medical Faculty Mannheim, University of Heidelberg, Square J5, 68159 Mannheim, Germany
[12] Department of Psychology, School of Social Sciences, University of Mannheim, 68131 Mannheim, Germany
[13] NeuroSpin, CEA, Université Paris-Saclay, F-91191, Gif-sur-Yvette, France
[14] Departments of Psychiatry and Psychology, University of Vermont, 05405 Burlington, Vermont, USA
[15] Sir Peter Mansfield Imaging Centre School of Physics and Astronomy, University of Nottingham, University Park, Nottingham, United Kingdom
[16] Physikalisch-Technische Bundesanstalt (PTB), Abbestr. 2 – 12, Berlin, Germany
[17] Institut National de la Santé et de la Recherche Médicale, INSERM Unit 1000 "Neuroimaging & Psychiatry", University Paris Sud, University Paris Descartes – Sorbonne Paris Cité; and Maison de Solenn, Paris, France
[18] Institut National de la Santé et de la Recherche Médicale, INSERM Unit 1000 "Neuroimaging & Psychiatry", University Paris Sud, University Paris Descartes; Sorbonne Université; and AP-HP, Department of Child and Adolescent Psychiatry, Pitié-Salpêtrière Hospital, Paris, France
[19] Bloorview Research Institute, Holland Bloorview Kids Rehabilitation Hospital and Departments of Psychology and Psychiatry, University of Toronto, Toronto, Ontario, M6A 2E1, Canada
[20] Department of Child and Adolescent Psychiatry and Psychotherapy, University Medical Centre Göttingen, von-Siebold-Str. 5, 37075, Göttingen, Germany
[21] Department of Psychiatry and Neuroimaging Center, Technische Universität Dresden, Dresden, Germany
[22] School of Psychology and Global Brain Health Institute, Trinity College Dublin, Ireland

Abstract

Recent large-scale, genome-wide association studies (GWAS) have identified hundreds of genetic loci associated with general intelligence. The cumulative influence of these loci on brain structure is unknown. We examined if cortical morphology mediates the relationship between GWAS-derived polygenic scores

for intelligence (PS_i) and *g*-factor. Using the effect sizes from one of the largest GWAS meta-analysis on general intelligence to date, PS_i were calculated among ten p-value thresholds. PS_i was assessed for the association with *g*-factor performance, cortical thickness (CT), and surface area (SA) in two large imaging-genetics samples (IMAGEN N=1,651; IntegraMooDS N=742). PS_i explained up to 5.1% of the variance of *g*-factor in IMAGEN ($F_{1,1640}$=12.2-94.3; P<0.005), and up to 3.0% in IntegraMooDS ($F_{1,725}$=10.0-21.0; P<0.005). The association between polygenic scores and *g*-factor was partially mediated by SA and CT in prefrontal, anterior cingulate, insula, and medial temporal cortices in both samples ($P_{FWER\text{-}corrected}$<0.005). The variance explained by mediation was up to 0.75% in IMAGEN and 0.77% in IntegraMooDS. Our results provide evidence that cumulative genetic load influences *g*-factor via cortical structure. The consistency of our results across samples suggests that cortex morphology could be a novel potential biomarker for neurocognitive dysfunction that are among the most intractable psychiatric symptoms.

Introduction

General intelligence (*g*-factor) is the primary component and predictor of performance on diverse psychometric tasks (Carroll 1993; Gray and Thompson 2004). These neurocognitive tasks are intercorrelated with one component consistently predicting approximately 40-45% of the variance (Carroll 1993; Jensen 1998a). Some life outcomes correlate with *g*-factor including physical and mental health, as well as job performance (Strenze 2007; Deary et al. 2018). Full-scale IQ measures and *g*-factor are distinct measures of intelligence in that IQ results from summation of standardized scores across several tests. These

measures are generally highly correlated. However, *g*-factor is an important component of IQ, but IQ is a specific mixture of cognitive abilities and skills that may not be represented by *g*-factor (Colom et al. 2002).

Cortical brain volumes are associated with *g*-factor (Thompson et al. 2001; Posthuma et al. 2002; Haier et al. 2004; Mcdaniel 2005). Although global effects have been reported, *g*-factor performance is most commonly associated with the dorsolateral prefrontal cortex (DLPFC), medial temporal lobes, anterior and posterior cingulate, and inferior parietal lobes (Haier et al. 2004; Toga and Thompson 2005; Narr et al. 2006; Basten et al. 2015). The heritability observed in *g*-factor and IQ may be shared among volumetric measures of cortical structure (Posthuma et al. 2002; Davies et al. 2018a; Elliott, Sharp, et al. 2018; Savage et al. 2018), and potentially epigenetic variation (Kaminski et al. 2018). However, the association with cortical volume and *g*-factor may be more complex as cortical thickness (CT) and surface area (SA) have distinct genetic contributions and developmental trajectories (Panizzon et al. 2009; Winkler et al. 2010; Hogstrom et al. 2013; Jha et al. 2018). CT and SA also have been associated with intelligence throughout the lifespan (Narr et al. 2006; Karama et al. 2011; Schnack et al. 2015; Schmitt et al. 2019). In particular, changes in CT in frontotemporal and inferior parietal regions during development have been shown to mediate the heritability of IQ. The heritability of *g*-factor has also been associated with brain volume differences in the same cortical regions, and these regions may partially share the genetic influences of neuropsychiatric disorders on brain structure (Toga and Thompson 2005).

The interindividual differences in *g*-factor performance have significant genetic and environmental contributions (Deary et al. 2009; Plomin et al. 2012). A conservative estimate for the heritability of *g*-factor is approximately 40% (Bouchard and McGue 1981; Deary et al. 2010; Haworth et al. 2010; Plomin and Deary 2015; Kaminski et al. 2018). Until recently, the contribution of common genetic variants accounting for this heritability was unclear. Several smaller GWAS identified tens of independent genetic loci associated with cognitive functioning (Davies et al. 2011, 2015, 2016; Benyamin et al. 2014; Kirkpatrick et al. 2014; Lencz et al. 2014; Lam et al. 2017; Sniekers et al. 2017; Trampush et al. 2017). More recently, a large genome-wide association meta-analysis uncovered 205 associated genomic loci and 1,016 genes that were statistically related to general intelligence in 269,867 participants (Savage et al. 2018). Another

study with large sample overlap with Savage et al. (2018), identified 148 independent loci and 709 genes influencing general cognitive function in 300,486 individuals (Davies et al. 2018b). Polygenic scores based on the recent GWAS studies explained approximately 2.0-5.2% of the variance in general intelligence (Davies et al. 2018b; Savage et al. 2018). There was also a robust genetic correlation, but with small effect size (r_g~-0.20), of polygenic scores for intelligence with neuropsychiatric disorders with prominent cognitive symptoms including schizophrenia (SCZ) (Ohi et al. 2018; Savage et al. 2018). It has been reported that the genetic correlation with general cognitive function may be protective or mitigate the diagnosis of psychiatric disorders (Lam et al. 2017; Sniekers et al. 2017; Trampush et al. 2017; Davies et al. 2018b; Savage et al. 2018). These genetic findings represent an important step to further elucidating the architecture of human intelligence and potential neurobiological mechanisms underlying cognitive impairment in psychiatric disorders.

Lower *g*-factor scores and IQ impairment have been reported among many neuropsychiatric disorders including SCZ (Heinrichs and Zakzanis 1998; Heaton et al. 2001), bipolar disorder (BPD) (Bora and Pantelis 2015), major depressive disorder (MDD) (Rock et al. 2014), attention deficit hyperactivity disorder (Hill et al. 2016), and autism spectrum disorder (ASD) (Millan et al. 2012). The neurocognitive domains contributing to lower *g*-factor scores vary among individuals and clinical subpopulations of these diseases. Moreover, the causes of neurocognitive impairment may be different between these disorders. For instance, an MDD patient may have dysfunction due an acute depressive episode in contrast to persistent cognitive symptoms in some chronic schizophrenia patients. Among psychiatric patients, neurocognitive symptoms have a negative impact on quality of life, social functioning, and occupational functioning (Green 2006; McIntyre et al. 2013). Cognitive impairments are particularly severe in some patients with ASD and SCZ in which cognitive deficits are a core feature of the disorders that are highly prevalent, manifest early, are relatively stable over time, and correlate with overall symptom severity (Seidman 2006; Savilla et al. 2008; Hill et al. 2016). Impairment is also present in first-degree relatives of patients suggesting a genetic component that is not a downstream effect of the disease process (Clark et al. 2005; Snitz et al. 2006; Bora

et al. 2009; Gau and Shang 2010; Rommelse et al. 2011). Therefore, *g*-factor has been argued to be an important endophenotype among psychiatric populations (e.g. Burdick et al. 2009).

In the present study, we used genome-wide, whole-brain neuroimaging, and neurocognitive performance data from two large independent samples: the naturalistic adolescent development cohort IMAGEN study (N=1,651), and the cross-psychiatric disorder IntegraMooDS sample (N=742) that includes healthy controls, as well as patients and first-degree relatives of patients with MDD, BPD, and SCZ. Our primary goal was to investigate the mechanistic relationship among the polygenic intelligence scores (PS_i), derived from the Savage et al. 2018 intelligence, wave 2 study (Savage et al. 2018), cortical structure, and *g*-factor performance which requires a number of intermediary steps. First, we aimed to validate the association between polygenic scores and *g*-factor. Second, we assessed the association of *g*-factor performance with vertex-wise measures of CT and SA. Third, we established which PS_i (thresholds ranging from $P_T<5.0\times10^{-8}$ to $P_T=1.0$) were associated with CT and SA. Last, we aimed to use vertex-wise putative causal models to assess if the association between PS_i and *g*-factor performance was mediated by cortical brain structure in youths, adults, relatives of patients, and patients.

Materials and Methods

Subjects

We analyzed two independent samples with neuroimaging, neurocognitive and genome-wide genotype data. The first sample (IMAGEN; www.imagen-europe.com; N=1,651) is a large-scale, longitudinal European imaging genetics study. It is a community-based sample of adolescents with Caucasian origin that was collected at eight different sites in Europe: Berlin, Germany (N=214); Dresden, Germany (N=239); Dublin, Ireland (N=154); Hamburg, Germany (N=215); London, England (N=186); Mannheim, Germany (N=192); Nottingham, England (N=257); and Paris, France (N=194). The average age was 13.9 ± 0.45 including 817 males and 834 females. A detailed description of the IMAGEN sample has been provided in earlier publications (Schumann et al. 2010; Kaminski et al. 2018). The ethics committees approved the

study among clinical sites. Legal guardians of participants provided written informed consent prior to commencement of the study.

The newly completed, cross-psychiatric disorder IntegraMooDS sample (N=742) consists of healthy controls (N=339), first degree relatives of MDD (rel-MDD; N=91), BPD (rel-BPD; N=69) and SCZ (rel-SCZ; N=67), and independent subgroups of patients with MDD (pat-MDD; N=67), BPD (pat-BPD; N=60), and SCZ (pat-SCZ; N=50; Table S1). The Structured Clinical Interview of the Diagnostic and Statistical Manual of Mental Disorders (DSM-IV) Axis-I Disorders (SCID-I) (First and Spitzer 2002) was used to confirm diagnosis of patients and to ensure that relatives and controls never suffered from a psychiatric disorder. Symptom severity was assessed using the SCL-90-R (Derogatis 1979) (Table S1). All participants reported having grandparents of European origin. Medication information is listed in Table S2. Data of IntegraMooDS participants was collected across three different German research institutions: Central Institute of Mental Health at the University of Heidelberg, Mannheim; Department of Psychiatry and Psychotherapy, University of Bonn, Bonn; and the Department of Psychiatry and Psychotherapy at Charité-Universitätsmedizin Berlin. The ethics committees of the participating centers approved the study and all participants provided written informed consent prior to commencement of the study. IMAGEN and IntegraMooDS were both conducted in accordance with the Declaration of Helsinki.

General Intelligence

Using standard methods (Spearman 1904; Mackintosh 2011; Davies et al. 2016; Savage et al. 2018), *g*-factor was defined as the first principal component among psychometric neurocognitive batteries encompassing multiple dimensions of cognitive functioning. Since IMAGEN and IntegraMooDS have different neurocognitive batteries, we conducted a principal component analysis (PCA) of the different cognitive tests available and selected the first unrotated component independently in each sample. In IMAGEN, *g*-factor was calculated from the WISC-IV (Feis 2010) including: matrix reasoning, block design, digit span backward and forward, similarities and vocabulary. In IntegraMooDS, we conducted PCA from the Hamburg-Wechsler Adult Intelligence Scale (HAWIE-R) (Wechsler 2008) subtests digit

span memory test (forwards and backwards), matrix reasoning, digit symbol and additional neurocognitive tests including verbal fluency (Aschenbrenner et al. 2000), verbal intelligence (Lehrl 1993), verbal learning and memory (Helmstaedter 2001), trail making test version a and b (Giovagnoli et al. 1996), and d2 concentration performance (Brickenkamp and Zillmer 1998). In both samples, the factor loadings of individual neurocognitive tests followed a typical pattern (Deary et al. 2010) and correlated highly with the extracted *g*-factor (all r>0.47; Figure S1). In general, *g*-factor scores are relatively stable even when calculated from a variety of cognitive tests (Jensen 1998b). For instance, *g*-factor scores obtained from different domains of cognitive tests correlate highly (Johnson et al. 2004, >0.98; 2008). In previous studies, *g*-factor generally accounts for 40% or more of the variance across different cognitive domains (Carroll and B. 1993; Deary et al. 2010). A detailed description of the different neuropsychological tests used in both samples is shown in the intelligence measures section of the Supplementary Material.

Genetics

Quality control, imputation and analysis of the genetic data for both the IMAGEN and IntegraMooDS samples was performed according to the standards of the Psychiatric Genomics Consortium (PGC; http://www.med.unc.edu/pgc; for further details see Supplementary Material, Genetics section). IMAGEN was a minor contribution to the original study conducted by Savage et al. (2018). To avoid bias, we were provided with the summary statistics by the authors excluding IMAGEN. This resulted in 268,524 individuals from the original GWAS with 9,270,275 SNPs instead of the 269,867 individuals included in the publication. Polygenic scores are used to summarize genome-wide effects among sets of genetic variants that may not achieve significance alone in large-scale association studies (Dudbridge 2013). Among genetically complex phenotypes, in which thousands of genetic polymorphisms may be contributing to the trait, these aggregated polygenic scores increase the predictive power that would not be achievable by a single variant alone (Dudbridge 2013). We used the latest general intelligence meta-analysis conducted by Savage et al. (2018) to calculate PS_i for each individuals in both samples as the weighted sum of the alleles associated with lower general intelligence. For each individual, we calculated ten PS_i deciles at p-value

thresholds ranging from p=1 to $p<0.5x10^{-8}$. Our thresholds, and the method in general, are standard among PGC publications (For further details, Supplementary Material, Genetics section) (Ripke et al. 2014; Cross-Disorder Group of the PGC 2013; Purcell et al. 2009). Genetic population stratification was assessed among the first four genetic principal components (IMAGEN: Figure S3; IntegraMooDS: Figure S4).

Image Acquisition

In IMAGEN, the image acquisition parameters and preprocessing steps have been described in detail in a prior publication (Schumann et al. 2010), and they are summarized in the image acquisition section of the Supplementary Material. In IntegraMooDS, scans were acquired using three Siemens Trio 3T MR (Siemens, Erlangen, Germany) scanners at Charité Universitätsmedizin Berlin, at the Life and Brain Center of the University of Bonn, and at the Zentralinstitut für seelische Gesundheit, Mannheim. Image acquisition parameters and processing of structural images are described in detail in prior publications (Lett et al. 2017; Vogel et al. 2018), and in the methods section of the Supplementary Material.

Statistical Analysis

Our statistical models were different in IMAGEN and IntegraMooDS. In IMAGEN, we included sex, age, site and the top four principal components (PCs) from the population stratification analysis as covariates. In IntegraMooDS, we additionally included the subgroups (healthy controls, rel-MDD, rel-BPD, rel-SCZ, pat-MDD, pat-BPD, and pat-SCZ) as covariates along with sex, age, site, and the top four PCs from the population stratification analysis. In follow-up analyses, we determined if we should be including the cross-diagnostic subgroups in IntegraMooDS as an interacting variable with each PS_i for both the main effects (i.e. PS_i on cortical structure), as well as the mediation effects (i.e. PS_i on *g*-factor via cortical structure). In both samples, linear regression was applied to investigate the association between PS_i and general intelligence. In IntegraMooDS, we followed-up this analysis examining PS_i by subgroup interactions.

Neuroimaging analysis

For vertex-wise analyses of cortical surfaces, the TFCE_mediation toolbox (Lett et al. 2017) was used (https://github.com/trislett/TFCE_mediation). The toolbox performs threshold-free cluster enhancement (TFCE) transformation on vertex-wise statistic images (Smith and Nichols, 2009). Significance of the TFCE transformed statistic image is assessed via permutation testing after correcting for family-wise error rate ($P_{FWER\text{-}corrected}$). The toolbox also allows for cortex-wise mediation analyses. For all neuroimaging analyses, significance was determined after 10,000 permutations at a $P_{FWER\text{-}corrected}<0.05$ and $P_{FWER\text{-}corrected}<0.005$ for analyses that included PS_i.

Cortex-wise mediation is explained in detail in the Supplementary Material, as well as in prior publications (Lett et al. 2016, 2017, 2018). This analysis allowed us to determine if the associations between PS_i and *g*-factor were independent of differences in SA and CT, or if SA and CT were mediating the effect. The mediation models in IMAGEN and IntegraMooDS were performed with PS_i as independent variable, vertex-wise SA or CT were the mediator variables, and *g*-factor was the dependent variable. At each vertex, the indirect effect was assessed using the Sobel Test Z-statistic (Sobel 1986). The Z-statistic images then underwent TFCE, and significance of cortex-wise mediation was determined after 10,000 permutations.

Post hoc estimation of effect sizes

To estimate the degree of partial mediation, we used the effect sizes (partial η^2) of the top cluster from the vertex-wise mediation analyses among all significant PS_i thresholds. We calculated the direct effect (PS_i on *g*-factor), the effect of PSi on the mean cluster values, the effect of the mean cluster values on *g*-factor, and the indirect effect of PS_i on *g*-factor including the top clusters as additional covariates. Furthermore, we calculated the percentage of the explainable variance (see formula below) in *g*-factor performance that is explained by the indirect effect (see Table S9). Neuroimaging *post hoc* effects estimations are inflated; however, this bias is reduced in larger sample sizes (Reddan et al. 2017; Geuter et al. 2018).

$$Percentage\ of\ explainable\ variance = \frac{partial\ \eta^2\ direct\ effect - partial\ \eta^2\ indirect\ effect}{partial\ \eta^2\ direct\ effect} \times 100$$

Results

General intelligence

In IMAGEN, *g*-factor explained 41.1% variance, and 41.7% of the variance in IntegraMooDS (Figure S1). In both samples, *g*-factor explained a similar amount of variance across various cognitive tests (Table S3; Figure S2). Within IntegraMooDS, *g*-factor was significantly different between subgroups ($F_{6,726}$=9.34, P=1.8x10^{-9}, Figure S5). Pairwise comparisons revealed that *g*-factor was significantly lower in rel-SCZ, pat-BPD and pat-SCZ compared to healthy controls, with the greatest difference in pat-SCZ compared to control subjects (Table S4).

Polygenic intelligence score

In both samples, PS_1 to PS_{10} correlated positively with each other after correction for multiple testing indicating a relatively high degree of collinearity among PS_i (IMAGEN: r=0.23-0.99, P<1.2x10^{-20}; IntegraMooDS: r=0.30-0.99, P<8.5x10^{-17}; Figure S6). In IntegraMooDS, the PS_1 to PS_{10} did not differ significantly between subgroups ($F_{6,727}$=0.33-1.86, P>0.05).

Association of polygenic scores with general intelligence

In the IMAGEN sample, PS_1 to PS_{10} were associated with *g*-factor with PS_6 to PS_8 explaining approximately 5.1% of the variance ($F_{1,1640}$=12.23-94.30; P<0.005; Figure 1). In the IntegraMooDS sample, PS_2 to PS_{10} were associated with *g*-factor with PS_5 explaining 3.0% of the variance ($F_{1,725}$= 9.99-20.98; P<0.005; Figure 1). In follow-up analyses, we included the interaction between PS_i and IntegraMooDS subgroups. There were no significant subgroup by PS_i interactions on *g*-factor at all PS_i thresholds ($F_{6,720}$=0.31-1.03, P>0.05).

Association among *g*-factor, cortical thickness and surface area

In IMAGEN, vertex-wise analysis of CT and SA revealed a positive association with *g*-factor throughout the cortex ($P_{FWER\text{-}corrected}$<0.05; Figure S7). This global effect was also observed in IntegraMooDS where increased CT and SA were associated with *g*-factor performance ($P_{FWER\text{-}corrected}$<0.05; Figure S7).

Association of polygenic scores and brain structure

Cortical Thickness

Within IMAGEN, PS_3 to PS_8 ($P_T<1.0x10^{-4}$ to $P_T<0.2$) were associated with higher CT ($P_{FWER\text{-}corrected}<0.005$; Table 1, Table S5) in the prefrontal cortices, anterior cingulate, insula, medial temporal cortex, and inferior parietal cortex (Figure S8 for PS_4). Within the IntegraMooDS sample, PS_2, PS_4, and PS_5 were associated with higher CT in similar regions as in IMAGEN (bilateral prefrontal cortex, anterior cingulate, insula, temporal cortex and inferior parietal cortex; $P_{FWER\text{-}corrected}<0.005$; Table 1, Table S5, Figure S8 for PS_4 vertex-wise results). Vertex-wise results for PS_i scores at $P_{FWER\text{-}corrected}<0.05$ and $P_{FWER\text{-}corrected}<0.005$ are available in the Supplementary Material under Online Vertex-wise Results. In follow-up analysis, there was no significant PS_i by subgroup interaction in the IntegraMooDS sample ($P_{FWER\text{-}corrected}>0.05$).

Surface Area

In IMAGEN, higher PS_3 to PS_5 were associated with larger SA ($P_{FWER\text{-}corrected}<0.005$; Table 1). The positive association between PS_i and SA was prominently observed in the frontal cortices, including bilateral DLPFC, as well as the anterior cingulate, insula, medial temporal cortex, and the inferior parietal cortex (Figure S8 for PS_4 vertex-wise results). In IntegraMooDS, higher PS_2, PS_4, PS_5, and PS_8 were associated with larger SA in similar regions as in IMAGEN (prefrontal cortices, anterior cingulate, insula, temporal cortex and inferior parietal cortex) ($P_{FWER\text{-}corrected}<0.005$; Table 1; Table S6). Vertex-wise results for PS_i scores at $P_{FWER\text{-}corrected}<0.05$ and $P_{FWER\text{-}corrected}<0.005$ are available in the Supplementary Material under Online Vertex-wise Results. Follow-up analysis revealed that there were no significant PS_i by subgroup interactions in the IntegraMooDS sample ($P_{FWER\text{-}corrected}>0.05$).

Cortex-wise mediation analyses

Cortical Thickness

In IMAGEN, CT partially mediated the relationship between PS_3 to PS_8 and *g*-factor ($P_{FWER\text{-}corrected}<0.005$; Table 1; Table S7). The mediation was primarily in the prefrontal cortices, anterior cingulate, insula, medial temporal cortex, and inferior parietal cortex (Figure 2 for PS_4). Within the IntegraMooDS sample, CT

mediated the relationship between PS_2 to PS_5 and *g*-factor in similar regions as IMAGEN ($P_{FWER\text{-}corrected}<0.005$; Table 1; Table S7; Figure 2 for PS_4). Vertex-wise results for PS_i scores at $P_{FWER\text{-}corrected}<0.05$ and $P_{FWER\text{-}corrected}<0.005$ are available in the Supplementary Material under Online Vertex-wise Results. We did not include IntegraMooDS subgroup as an interacting variable in the mediation model because there was no significant PS_i by subgroup interaction on CT ($P_{FWER\text{-}corrected}>0.05$).

Surface Area

In IMAGEN, the association between PS_i and *g*-factor was partially mediated by SA, particularly in the prefrontal cortices, including bilateral DLPFC, as well as anterior cingulate, insula, medial temporal cortex, and inferior parietal cortex (Figure 3 for PS_4 vertex-wise results). SA mediated the relationship between PS_4 to PS_8 and *g*-factor ($P_{FWER\text{-}corrected}<0.005$; Table S8). Within the IntegraMooDS sample, SA mediated the relationship between PS_2 to PS_5 and PS_6 to PS_{10} and *g*-factor in similar regions as IMAGEN ($P_{FWER\text{-}corrected}<0.05$; Table 1; Table S8; Figure 3 for PS_4). Vertex-wise results for PS_i scores at $P_{FWER\text{-}corrected}<0.05$ and $P_{FWER\text{-}corrected}<0.005$ are available in the Supplementary Material under Online Vertex-wise Results. We did not include IntegraMooDS subgroup as an interacting variable in the mediation model because there was no significant PS_i by subgroup interaction on SA ($P_{FWER\text{-}corrected}>0.05$).

Post hoc estimation of the mediation effects

We estimated the *post hoc* effect sizes from the mean top cluster values of the vertex-wise mediation analyses (Table 1, Figures 2-3, and Tables S6-S8). For the direct effect, associations between PS_i and *g*-factor, the partial η^2 of the ranged from 0.007-0.054 in IMAGEN and 0.014-0.028 in IntegraMooDS (Figure 1, Table S9). The variance explained for PS_i, on CT ranged from partial η^2=0.009-0.017 in IMAGEN, and partial η^2=0.019-0.034 in IntegraMooDS, and the variance explained for PS_i on SA ranged from partial η^2=0.005-0.013 in IMAGEN, and partial η^2=0.012-0.023 in IntegraMooDS (Table S9).

The indirect effect of PS_i and *g*-factor via the top CT clusters ranged from partial η^2 = 0.0028 to 0.0075 in IMAGEN, and partial η^2=0.0019-0.0076 in IntegraMooDS (Table S9). Of the explainable variance in *g*-factor by PS_i, the indirect effect explained ranged between 10.7%-24.9% in IMAGEN, and 12.2%-41.0% in IntegraMooDS. The indirect effect of PS_i and *g*-factor via CT ranged from partial

η^2=0.0021-0.0065 in IMAGEN, and partial η^2=0.0029-0.0062 in IntegraMooDS (Table S9). Of the explainable variance in *g*-factor, the indirect effect of the SA explained between 6.3%-18.9% in IMAGEN, and 17.7%-32.3% in IntegraMooDS (Table S9).

Discussion

It has been reported that the genetic contribution to general intelligence is partially shared with the genetics of cortical structure (Grasby et al. 2018; Savage et al. 2018). To the best of our knowledge, we provide first direct evidence that the genetic influence of common variants on general intelligence is partially mediated by its intermediate effect on CT and SA. Individuals with higher PS_i scores, particularly at the P_T<0.001 threshold (PS_4), had higher CT and SA in the frontotemporal, inferior parietal, and anterior cingulate regions that putatively led to better *g*-factor performance. These results were remarkably consistent among 14-year-old adolescents in the IMAGEN sample, as well as among the adult subgroups of the IntegraMooDS sample, suggesting that PS_i may be independent of the subject population. Moreover, we potentially validate the functional effect of our SNP-derived PS_i since the cortical regions that mediate genetic effects on *g*-factor are similar to the regions associated with intelligence identified in twin-based heritability studies. All in all, we provide functional evidence that the cortical regions associated with the PS_i may be integral to inter-individual differences in *g*-factor performance.

Among the IMAGEN and IntegraMooDS samples, we found remarkably consistent associations among: (1) PS_i and *g*-factor, (2) PS_i and cortical structure, and (3) cortical structure and *g*-factor. We demonstrated consistent associations between PS_i and *g*-factor performance in IMAGEN and IntegraMooDS with variance explained maximizing around the P_T<0.001 threshold (PS_4). Importantly, it should be noted that we derived our PS_i from a subsample of the meta-analysis that excluded IMAGEN. We replicated the Savage et al. (2018) PS_i association with intelligence in the cross-disorder IntegraMooDS sample, and in both samples the maximum PS_i was around P_T<0.001 polygenic threshold (PS_4) (Savage et al. 2018). Importantly, PS_i was also robustly associated with CT and SA in prefrontal, medial temporal, anterior cingulate, parietal, and insular cortices in both samples even after correcting for ten PS_i thresholds

and FWER across all vertices (approximately 3 million vertices in total). The topography of these associations is consistent with regions that have been heavily implicated by structural and functional neuroimaging studies in neurocognitive capacity (Deary et al. 2010; Basten et al. 2015; Pietschnig et al. 2015). The associated regions are also consistent to previously reported areas that have high heritability and are associated with general intelligence (Thompson et al. 2001; Gray and Thompson 2004; Toga and Thompson 2005; Narr et al. 2006). Within our samples, there were brain-wide positive correlations among CT and SA and *g*-factor performance. The unspecific effect of cortex morphology on *g*-factor performance is consistent with recent meta-analytic data demonstrating robust associations between general cognitive function and total brain volume (Elliott, Belsky, et al. 2018). This result is also consistent with general associations with most structural MRI phenotypes (Ritchie et al. 2015) and intelligence including CT (Shaw et al. 2006; Karama et al. 2011) and SA (Lencz et al. 2014). Therefore, a natural question is if there is a latent association among these three correlations.

To date, the majority of neuroimaging and genetics studies examining cognition have focused on pairwise relationships among genetics-cognition, genetics-brain, or brain-cognition. We performed vertex-wise mediation analysis of CT and SA among ten PS_i thresholds in two independent samples linking genetics, brain structure and general intelligence. Our cortex-wise mediation findings are in-line with the few studies that have examined genetics-brain-cognition relationships. We observed a consistent mediation particularly in frontal regions, such as the DLPFC, as well as the anterior cingulate cortex, posterior cingulate cortex, and medial temporal lobes, where cortical structure mediated the effect of PS_i on *g*-factor. Our results are spatially similar to twin-based heritability studies. In virtually identical regions, cortical grey matter volume mediated the association of the genetic influence on *g*-factor (Gray and Thompson 2004). More recently, frontotemporal cortical thickness, as well as change in cortical thickness during adolescence were also demonstrated to mediate the genetic association with full-scale IQ (Schmitt et al. 2019). Therefore, the genetic influence estimated by GWAS meta-analysis derived PS_i or twin-based heritability both support a shared associations of genetics and brain structure on intelligence. Furthermore, a meta-analysis across four independent samples found a weak but consistent mediation effect among

polygenic scores derived from an education attainment GWAS (Davies et al. 2016), total brain volume, and cognitive performance (Elliott, Belsky, et al. 2018). These previous findings on total brain volume mediation are consistent with our results given the relatively strong, GWAS-derived, genetic correlation between intelligence and educational attainment (r_g~0.70) (Rietveld et al. 2013; Savage et al. 2018). Our mediation findings are also consistent with the association between intelligence and brain activation during cognitive demand in lateral prefrontal, insular, parietal, temporal, motor, as well as posterior and anterior cingulate regions (Basten et al. 2015; Hearne et al. 2016; Saxe et al. 2018). Since we observed a more specific mediation effect in frontotemporal, and insular regions, it could be speculated that the relatively weak total brain volume mediation could be too general of a phenotype.

There are some important limitations to this study. Mediation analyses inherently imply causal inference; however, we are cautious of this implication. We had a strong *a priori* hypothesis of the direction of our mediation models: genetics likely determine brain structure (and not vice versa), and brain structure likely determines *g*-factor; however, in both IMAGEN and IntegraMooDS the PS_i only explained 3-5% of the variance in *g*-factor performance. We are only explaining a portion of the genetic contribution to intelligence (for example, the SNP-based heritability of general intelligence is approximately 20% (Marioni et al. 2014; Davies et al. 2018b; Savage et al. 2018)). Moreover, while we observed widespread and strongly significant associations among CT, SA and *g*-factor, these structures explained only 2-3% of the variance of *g*-factor after including PS_i as a covariate. Together these explain why the maximum amount of the variance mediated by CT and SA was only around 0.7%. However, it should be noted that 0.7% represents 20-40% of the initial PS_i association with *g*-factor in IMAGEN and IntegraMooDS, respectively. While in the context of imaging-genetics studies of behavior phenotypes this amount of explained variance is not trivial, we cannot infer direct conclusions explaining *g*-factor performance. Therefore, our results should not be viewed as a causal gene-brain-behavior mechanism, but rather as an insight to cortical regions that directly related to PS_i and *g*-factor performance that are more specific than either of these associations alone. Further, our subgroups were too small to make definitive conclusions about the patient groups. Within IntegraMooDS, our results were consistent across patient and relative subgroups suggesting the

genetic association is independent from psychiatric diagnosis, nevertheless these results need to be confirmed in larger patient samples. Moreover, both our samples were of European descent; therefore, we are unable to assess the effect of PS_i in other ethnic subgroups. Last, there is a known interaction among age, surface area, cortical thickness and intelligence (Narr et al. 2006; Karama et al. 2014). We observed consistent genetic effects on cortical structure in adolescents and adults. However, a sample designed to assess across-the-lifespan effects would be needed to assess any neurodevelopmental effects.

Our findings support a direction of effect in which GWAS-derived PS_i effects cortical structure, which in turn, correlates with *g*-factor performance. In particular, it supports an intermediate role of cortical morphology in the relationship between cumulative genetic load for general intelligence and *g*-factor performance. Although polygenic scores are unlikely to account for all of the genetically explained variance in *g*-factor performance, PS_i appears to be an interesting factor collectively influencing cortical structure and neurocognition.

Funding

This research was supported by the German Ministry for Education and Research (BMBF) grants NGFNplus MooDS 01GS08148, e:Med program O1ZX1314B and O1ZX1314G as well as Forschungsnetz AERIAL 01EE1406A and 01EE1406B. Further, this work is supported by a NARSAD Distinguished Investigator Grant to H.W. and S.R.. B.O.V. is funded by BMBF Grant 01EE1407 and T.A.L. is funded by DFG grant Wa 1539/11-1, ER 724/4-1. Further, this work received support from the following sources: the European Union-funded FP6 Integrated Project IMAGEN (Reinforcement-related behaviour in normal brain function and psychopathology) (LSHM-CT- 2007-037286), the Horizon 2020 funded ERC Advanced Grant 'STRATIFY' (Brain network based stratification of reinforcement-related disorders) (695313), ERANID (Understanding the Interplay between Cultural, Biological and Subjective Factors in Drug Use Pathways) (PR-ST-0416-10004), BRIDGET (JPND: BRain Imaging, cognition Dementia and next generation GEnomics) (MR/N027558/1), the FP7 projects IMAGEMEND(602450; IMAging GEnetics for MENtal Disorders) and MATRICS (603016), the Innovative Medicine Initiative Project EU-AIMS (115300-2), the Medical Research Council Grant 'c-VEDA' (Consortium on Vulnerability to Externalizing Disorders and Addictions) (MR/N000390/1), the Swedish Research Council FORMAS, the Medical Research Council, the National Institute for Health Research (NIHR) Biomedical Research Centre at South London and Maudsley NHS Foundation Trust and King's College London, the Bundesministeriumfür Bildung und Forschung (BMBF grants 01GS08152; 01EV0711; eMED SysAlc01ZX1311A; Forschungsnetz AERIAL 01EE1406A, 01EE1406B), the Deutsche Forschungsgemeinschaft (DFG grants, SM 80/7-2, SFB 940/2), the Medical Research Foundation and Medical research council (grant MR/R00465X/1). Further support was provided by grants from: ANR (project AF12-NEUR0008-01 – WM2NA, and ANR-12-SAMA-0004), the Fondation de France, the Fondation pour la Recherche Médicale,

the Mission Interministérielle de Lutte-contre-les-Drogues-et-les-Conduites-Addictives (MILDECA), the Fondation pour la Recherche Médicale (DPA20140629802), the Fondation de l'Avenir, Paris Sud University IDEX 2012; the National Institutes of Health, Science Foundation Ireland (16/ERCD/3797), U.S.A. (Axon, Testosterone and Mental Health during Adolescence; RO1 MH085772-01A1), and by NIH Consortium grant U54 EB020403, supported by a cross-NIH alliance that funds Big Data to Knowledge Centres of Excellence.

Acknowledgements

None

Conflicts of Interest

T.B. has served as an advisor or consultant to Bristol-Myers Squibb, Desitin Arzneimittel, Eli Lilly, Medice, Novartis, Pfizer, Shire, UCB, and Vifor Pharma; he has received conference attendance support, conference support, or speaking fees from Eli Lilly, Janssen McNeil, Medice, Novartis, Shire, and UCB; and he is involved in clinical trials conducted by Eli Lilly, Novartis, and Shire; the present work is unrelated to these relationships. M.M. has been a member of the scientific advisory boards for the Lundbeck Foundation and Robert-Bosch-Stiftung, is a member of the Medical-Scientific Editorial Office of Deutsches Ärzteblatt, has received travel support from Shire Deutschland GmbH, and receives a salary from and holds shares in Life and Brain GmbH. A.M-L. discloses speaker and/or advisor or authorship fees from Astra Zeneca, Servier, Bristol-Myers Squibb GmbH & Co.KGaA, Desitin Arzneimittel GmbH, Defined Health, F. Hoffmann-La Roche Ltd., Lilly Deutschland GmbH, Gerson Lehrmann Group (GLG), Pricespective, Elsevier, Alexza Pharmaceuticals Inc., Outcome Sciences Inc., Pfizer Pharma GmbH, Janssen-Cilag EMEA. H.W. received a speaker honorarium from Servier (2014). The other authors report no financial interest or potential conflicts of interest.

Online Supplementary Material

- Online Vertex-wise Results (github.com/bobvogel/g-factor-mediation)

References

Aschenbrenner S, Tucha O, Lange KW. 2000. Regensburger Wortflüssigkeits-Test: RWT ; Handanweisung.

Basten U, Hilger K, Fiebach CJ. 2015. Where smart brains are different: A quantitative meta-analysis of functional and structural brain imaging studies on intelligence. Intelligence. 51:10–27.
Benyamin B, Pourcain B, Davis OS, Davies G, Hansell NK, Brion M-JA, et al. 2014. Childhood intelligence is heritable, highly polygenic and associated with FNBP1L. Mol Psychiatry. 19:253–258.
Bora E, Pantelis C. 2015. Meta-analysis of Cognitive Impairment in First-Episode Bipolar Disorder: Comparison With First-Episode Schizophrenia and Healthy Controls. Schizophr Bull. 41:1095–1104.
Bora E, Yucel M, Pantelis C. 2009. Cognitive endophenotypes of bipolar disorder: a meta-analysis of neuropsychological deficits in euthymic patients and their first-degree relatives. J Affect Disord. 113:1–20.
Bouchard TJ Jr, McGue M. 1981. Familial studies of intelligence: a review. Science. 212:1055–1059.
Brickenkamp R, Zillmer E. 1998. The d2 test of attention. Hogrefe & Huber Pub.
Burdick KE, Gunawardane N, Woodberry K, Malhotra AK. 2009. The role of general intelligence as an intermediate phenotype for neuropsychiatric disorders. Cogn Neuropsychiatry. 14:299–311.
Carroll JB. 1993. Human Cognitive Abilities: A Survey of Factor-Analytic Studies. Cambridge University Press.
Carroll JB, B. CJ. 1993. Human Cognitive Abilities: A Survey of Factor-Analytic Studies. Cambridge University Press.
Clark L, Sarna A, Goodwin GM. 2005. Impairment of executive function but not memory in first-degree relatives of patients with bipolar I disorder and in euthymic patients with unipolar depression. Am J Psychiatry. 162:1980–1982.
Colom R, Abad FJ, Garcıa LF, Juan-Espinosa M. 2002. Education, Wechsler's full scale IQ, and g. Intelligence. 30:449–462.
Davies G, Armstrong N, Bis JC, Bressler J, Chouraki V, Giddaluru S, et al. 2015. Genetic contributions to variation in general cognitive function: a meta-analysis of genome-wide association studies in the CHARGE consortium (N=53949). Mol Psychiatry. 20:183–192.
Davies G, Lam M, Harris SE, Trampush JW, Luciano M, Hill WD, et al. 2018a. Study of 300,486 individuals identifies 148 independent genetic loci influencing general cognitive function. Nat Commun. 9:2098.
Davies G, Lam M, Harris SE, Trampush JW, Luciano M, Hill WD, et al. 2018b. Study of 300,486 individuals identifies 148 independent genetic loci influencing general cognitive function. Nat Commun. 9:2098.
Davies G, Marioni RE, Liewald DC, Hill WD, Hagenaars SP, Harris SE, et al. 2016. Genome-wide association study of cognitive functions and educational attainment in UK Biobank (N=112 151). Mol Psychiatry. 21:758–767.
Davies G, Tenesa A, Payton A, Yang J, Harris SE, Liewald D, et al. 2011. Genome-wide association studies establish that human intelligence is highly heritable and polygenic. Mol Psychiatry. 16:996–1005.
Deary IJ, Harris SE, Hill WD. 2018. What genome-wide association studies reveal about the association between intelligence and physical health, illness, and mortality. Curr Opin Psychol. 27:6–12.
Deary IJ, Johnson W, Houlihan LM. 2009. Genetic foundations of human intelligence. Hum Genet. 126:215–232.
Deary IJ, Penke L, Johnson W. 2010. The neuroscience of human intelligence differences. Nat Rev Neurosci. 11:201–211.
Derogatis LR. 1979. Symptom Checklist-90-Revised (SCL-90-R). Lyndhurst, NJ: NCS Pearson.
Dudbridge F. 2013. Power and predictive accuracy of polygenic risk scores. PLoS Genet. 9:e1003348.
Elliott ML, Belsky DW, Anderson K, Corcoran DL, Ge T, Knodt A, et al. 2018. A Polygenic Score for Higher Educational Attainment is Associated with Larger Brains. Cereb Cortex.
Elliott, Sharp K, Alfaro-Almagro F, Shi S, Miller KL, Douaud G, et al. 2018. Genome-wide association studies of brain imaging phenotypes in UK Biobank. Nature. 562:210–216.

Feis YF. 2010. Wechsler Intelligence Scale for Children-IV (WISC-IV). In: Encyclopedia of Cross-Cultural School Psychology. p. 1030–1032.
First MB, Spitzer RL. 2002. Gibbon Miriam, and Williams, Janet BW Structured Clinical Interview for DSM-IV-TR Axis I Disorders, Research Version, Non-patient Edition. SCIDI/NP) New York: Biometrics Research, New York State Psychiatric Institute.
Gau SS-F, Shang C-Y. 2010. Executive functions as endophenotypes in ADHD: evidence from the Cambridge Neuropsychological Test Battery (CANTAB). J Child Psychol Psychiatry. 51:838–849.
Geuter S, Qi G, Welsh RC, Wager TD, Lindquist MA. 2018. Effect Size and Power in fMRI Group Analysis.
Giovagnoli AR, Del Pesce M, Mascheroni S, Simoncelli M, Laiacona M, Capitani E. 1996. Trail making test: normative values from 287 normal adult controls. Ital J Neurol Sci. 17:305–309.
Grasby KL, Jahanshad N, Painter JN, Colodro-Conde L, Bralten J, Hibar DP, et al. 2018. The genetic architecture of the human cerebral cortex. bioRxiv.
Gray JR, Thompson PM. 2004. Neurobiology of intelligence: science and ethics. Nat Rev Neurosci. 5:471–482.
Green MF. 2006. Cognitive impairment and functional outcome in schizophrenia and bipolar disorder. J Clin Psychiatry. 67:e12.
Haier RJ, Jung RE, Yeo RA, Head K, Alkire MT. 2004. Structural brain variation and general intelligence. Neuroimage. 23:425–433.
Haworth CMA, Wright MJ, Luciano M, Martin NG, de Geus EJC, van Beijsterveldt CEM, et al. 2010. The heritability of general cognitive ability increases linearly from childhood to young adulthood. Mol Psychiatry. 15:1112–1120.
Hearne LJ, Mattingley JB, Cocchi L. 2016. Functional brain networks related to individual differences in human intelligence at rest. Sci Rep. 6:32328.
Heaton RK, Gladsjo JA, Palmer BW, Kuck J, Marcotte TD, Jeste DV. 2001. Stability and Course of Neuropsychological Deficits in Schizophrenia. Arch Gen Psychiatry. 58:24–32.
Heinrichs RW, Zakzanis KK. 1998. Neurocognitive deficit in schizophrenia: a quantitative review of the evidence. Neuropsychology. 12:426–445.
Helmstaedter C. 2001. VLMT Verbaler Lern- und Merkfähigkeitstest: Manual.
Hill WD, Davies G, CHARGE Cognitive Working Group, Liewald DC, McIntosh AM, Deary IJ. 2016. Age-Dependent Pleiotropy Between General Cognitive Function and Major Psychiatric Disorders. Biol Psychiatry. 80:266–273.
Hogstrom LJ, Westlye LT, Walhovd KB, Fjell AM. 2013. The structure of the cerebral cortex across adult life: age-related patterns of surface area, thickness, and gyrification. Cereb Cortex. 23:2521–2530.
Jensen AR. 1998a. The g factor: The science of mental ability. Praeger Westport, CT.
Jensen AR. 1998b. Human evolution, behavior, and intelligence. The g factor: The science of mental ability. Westport, CT, US.
Jha SC, Xia K, Schmitt JE, Ahn M, Girault JB, Murphy VA, et al. 2018. Genetic influences on neonatal cortical thickness and surface area. Hum Brain Mapp. 39:4998–5013.
Johnson W, Bouchard TJ, Krueger RF, McGue M, Gottesman II. 2004. Corrigendum to “Just one g: consistent results from three test batteries.” Intelligence.
Johnson W, Nijenhuis J te, Bouchard TJ. 2008. Still just 1 g: Consistent results from five test batteries. Intelligence. 36:81–95.
Kaminski JA, Schlagenhauf F, Rapp M, Awasthi S, Ruggeri B, Deserno L, et al. 2018. Epigenetic variance in dopamine D2 receptor: a marker of IQ malleability? Transl Psychiatry. 8:169.
Karama S, Bastin ME, Murray C, Royle NA, Penke L, Muñoz Maniega S, et al. 2014. Childhood cognitive ability accounts for associations between cognitive ability and brain cortical thickness in old age. Mol Psychiatry. 19:555–559.
Karama S, Colom R, Johnson W, Deary IJ, Haier R, Waber DP, et al. 2011. Cortical thickness correlates of specific cognitive performance accounted for by the general factor of intelligence in healthy

children aged 6 to 18. Neuroimage. 55:1443–1453.
Kirkpatrick RM, McGue M, Iacono WG, Miller MB, Basu S. 2014. Results of a "GWAS Plus:" General Cognitive Ability Is Substantially Heritable and Massively Polygenic. PLoS One. 9:e112390.
Lam M, Trampush JW, Yu J, Knowles E, Davies G, Liewald DC, et al. 2017. Large-Scale Cognitive GWAS Meta-Analysis Reveals Tissue-Specific Neural Expression and Potential Nootropic Drug Targets. Cell Rep. 21:2597–2613.
Lehrl S. 1993. Mehrfachwahl-Wortschatz-Intelligenztest: MWT-B ; [Manual zum MWT-B].
Lencz T, Knowles E, Davies G, Guha S, Liewald DC, Starr JM, et al. 2014. Molecular genetic evidence for overlap between general cognitive ability and risk for schizophrenia: a report from the Cognitive Genomics consorTium (COGENT). Mol Psychiatry. 19:168–174.
Lett TA, Kennedy JL, Radhu N, Dominguez LG, Chakravarty MM, Nazeri A, et al. 2016. Prefrontal White Matter Structure Mediates the Influence of GAD1 on Working Memory. Neuropsychopharmacology. 41:2224–2231.
Lett TA, Mohnke S, Amelung T, Brandl EJ, Schiltz K, Pohl A, et al. 2018. Multimodal neuroimaging measures and intelligence influence pedophile child sexual offense behavior. Eur Neuropsychopharmacol. 28:818–827.
Lett TA, Waller L, Tost H, Veer IM, Nazeri A, Erk S, et al. 2017. Cortical surface-based threshold-free cluster enhancement and cortexwise mediation. Hum Brain Mapp. 38:2795–2807.
Mackintosh NJ. 2011. IQ and Human Intelligence. Oxford University Press.
Marioni RE, Davies G, Hayward C, Liewald D, Kerr SM, Campbell A, et al. 2014. Molecular genetic contributions to socioeconomic status and intelligence. Intelligence. 44:26–32.
Mcdaniel M. 2005. Big-brained people are smarter: A meta-analysis of the relationship between in vivo brain volume and intelligence. Intelligence. 33:337–346.
McIntyre RS, Cha DS, Soczynska JK, Woldeyohannes HO, Gallaugher LA, Kudlow P, et al. 2013. Cognitive deficits and functional outcomes in major depressive disorder: determinants, substrates, and treatment interventions. Depress Anxiety. 30:515–527.
Millan MJ, Agid Y, Brüne M, Bullmore ET, Carter CS, Clayton NS, et al. 2012. Cognitive dysfunction in psychiatric disorders: characteristics, causes and the quest for improved therapy. Nat Rev Drug Discov. 11:141–168.
Narr KL, Woods RP, Thompson PM, Szeszko P, Robinson D, Dimtcheva T, et al. 2006. Relationships between IQ and Regional Cortical Gray Matter Thickness in Healthy Adults. Cereb Cortex. 17:2163–2171.
Ohi K, Sumiyoshi C, Fujino H, Yasuda Y, Yamamori H, Fujimoto M, et al. 2018. Genetic Overlap between General Cognitive Function and Schizophrenia: A Review of Cognitive GWASs. Int J Mol Sci. 19:3822.
Panizzon MS, Fennema-Notestine C, Eyler LT, Jernigan TL, Prom-Wormley E, Neale M, et al. 2009. Distinct genetic influences on cortical surface area and cortical thickness. Cereb Cortex. 19:2728–2735.
Pietschnig J, Penke L, Wicherts JM, Zeiler M, Voracek M. 2015. Meta-analysis of associations between human brain volume and intelligence differences: How strong are they and what do they mean? Neurosci Biobehav Rev. 57:411–432.
Plomin R, Deary IJ. 2015. Genetics and intelligence differences: five special findings. Mol Psychiatry. 20:98–108.
Plomin R, DeFries JC, Knopik VS, Neiderhiser JM. 2012. Behavioral Genetics. Worth Publishers.
Posthuma D, De Geus EJC, Baaré WFC, Hulshoff Pol HE, Kahn RS, Boomsma DI. 2002. The association between brain volume and intelligence is of genetic origin. Nat Neurosci.
Reddan MC, Lindquist MA, Wager TD. 2017. Effect Size Estimation in Neuroimaging. JAMA Psychiatry. 74:207–208.
Rietveld CA, Medland SE, Derringer J, Yang J, Esko T, Martin NW, et al. 2013. GWAS of 126,559 individuals identifies genetic variants associated with educational attainment. Science. 340:1467–1471.

Ripke S, Neale BM, Corvin A, Walters JTR, Farh K-H, Holmans PA, et al. 2014. Biological insights from 108 schizophrenia-associated genetic loci. Nature. 511:421.
Ritchie SJ, Booth T, Valdés Hernández MDC, Corley J, Maniega SM, Gow AJ, et al. 2015. Beyond a bigger brain: Multivariable structural brain imaging and intelligence. Intelligence. 51:47–56.
Rock PL, Roiser JP, Riedel WJ, Blackwell AD. 2014. Cognitive impairment in depression: a systematic review and meta-analysis. Psychol Med. 44:2029–2040.
Rommelse NNJ, Geurts HM, Franke B, Buitelaar JK, Hartman CA. 2011. A review on cognitive and brain endophenotypes that may be common in autism spectrum disorder and attention-deficit/hyperactivity disorder and facilitate the search for pleiotropic genes. Neurosci Biobehav Rev. 35:1363–1396.
Savage JE, Jansen PR, Stringer S, Watanabe K, Bryois J, de Leeuw CA, et al. 2018. Genome-wide association meta-analysis in 269,867 individuals identifies new genetic and functional links to intelligence. Nat Genet. 50:912–919.
Savilla K, Kettler L, Galletly C. 2008. Relationships between cognitive deficits, symptoms and quality of life in schizophrenia. Aust N Z J Psychiatry. 42:496–504.
Saxe GN, Calderone D, Morales LJ. 2018. Brain entropy and human intelligence: A resting-state fMRI study. PLoS One. 13:e0191582.
Schmitt JE, Raznahan A, Clasen LS, Wallace GL, Pritikin JN, Lee NR, et al. 2019. The Dynamic Associations Between Cortical Thickness and General Intelligence are Genetically Mediated. Cereb Cortex.
Schnack HG, van Haren NEM, Brouwer RM, Evans A, Durston S, Boomsma DI, et al. 2015. Changes in thickness and surface area of the human cortex and their relationship with intelligence. Cereb Cortex. 25:1608–1617.
Schumann G, Loth E, Banaschewski T, Barbot A, Barker G, Büchel C, et al. 2010. The IMAGEN study: reinforcement-related behaviour in normal brain function and psychopathology. Mol Psychiatry. 15:1128–1139.
Seidman LJ. 2006. Neuropsychological functioning in people with ADHD across the lifespan. Clin Psychol Rev. 26:466–485.
Shaw P, Greenstein D, Lerch J, Clasen L, Lenroot R, Gogtay N, et al. 2006. Intellectual ability and cortical development in children and adolescents. Nature. 440:676–679.
Sniekers S, Stringer S, Watanabe K, Jansen PR, Coleman JRI, Krapohl E, et al. 2017. Genome-wide association meta-analysis of 78,308 individuals identifies new loci and genes influencing human intelligence. Nat Genet. 49:1107–1112.
Snitz BE, Macdonald AW 3rd, Carter CS. 2006. Cognitive deficits in unaffected first-degree relatives of schizophrenia patients: a meta-analytic review of putative endophenotypes. Schizophr Bull. 32:179–194.
Sobel ME. 1986. Some New Results on Indirect Effects and Their Standard Errors in Covariance Structure Models. Sociol Methodol. 16:159–186.
Spearman C. 1904. “General Intelligence,” Objectively Determined and Measured. Am J Psychol. 15:201.
Strenze T. 2007. Intelligence and socioeconomic success: A meta-analytic review of longitudinal research. Intelligence. 35:401–426.
Thompson PM, Cannon TD, Narr KL, van Erp T, Poutanen VP, Huttunen M, et al. 2001. Genetic influences on brain structure. Nat Neurosci. 4:1253–1258.
Toga AW, Thompson PM. 2005. GENETICS OF BRAIN STRUCTURE AND INTELLIGENCE. Annu Rev Neurosci. 28:1–23.
Trampush JW, Yang MLZ, Yu J, Knowles E, Davies G, Liewald DC, et al. 2017. GWAS meta-analysis reveals novel loci and genetic correlates for general cognitive function: a report from the COGENT consortium. Mol Psychiatry. 22:1651–1652.
Vogel BO, Lett TA, Erk S, Mohnke S, Wackerhagen C, Brandl EJ, et al. 2018. The influence of MIR137 on white matter fractional anisotropy and cortical surface area in individuals with familial risk for psychosis. Schizophr Res. 195:190–196.

Wechsler D. 2008. WAIS-IV Administration and Scoring Manual.
Winkler AM, Kochunov P, Blangero J, Almasy L, Zilles K, Fox PT, et al. 2010. Cortical thickness or grey matter volume? The importance of selecting the phenotype for imaging genetics studies. Neuroimage. 53:1135–1146.

Tables

	Cortical Thickness		Surface Area	
Main Effect	IMAGEN	IntegraMooDS	IMAGEN	IntegraMooDS
PS_1 ($P_T < 5.0 \times 10^{-8}$)	-	*	-	-
PS_2 ($P_T < 1.0 \times 10^{-6}$)	*	***	*	***
PS_3 ($P_T < 1.0 \times 10^{-4}$)	***	*	***	*
PS_4 ($P_T < 0.001$)	***	***	***	***
PS_5 ($P_T < 0.01$)	***	***	***	***
PS_6 ($P_T < 0.05$)	***	*	***	*
PS_7 ($P_T < 0.1$)	***	*	*	*
PS_8 ($P_T < 0.2$)	***	*	*	***
PS_9 ($P_T < 0.5$)	*	*	*	*
PS_{10} ($P_T < 1.0$)	*	*	-	*
Indirect Effect	IMAGEN	IntegraMooDS	IMAGEN	IntegraMooDS
PS_1 ($P_T < 5.0 \times 10^{-8}$)	-	***	-	-

PS_2 ($P_T < 1.0 \times 10^{-6}$)	*	***	*	***
PS_3 ($P_T < 1.0 \times 10^{-4}$)	***	***	***	***
PS_4 ($P_T < 0.001$)	***	***	***	***
PS_5 ($P_T < 0.01$)	***	***	***	***
PS_6 ($P_T < 0.05$)	***	*	***	*
PS_7 ($P_T < 0.1$)	***	*	***	***
PS_8 ($P_T < 0.2$)	***	*	***	***
PS_9 ($P_T < 0.5$)	*	*	*	***
PS_{10} ($P_T < 1.0$)	*	*	-	***

Table 1. Associations of polygenic scores for general intelligence and surface area as well as cortical thickness in IMAGEN and IntegraMooDS at two different thresholds, separately for main effects and mediation analyses (indirect effect). *, represents the familywise error rate corrected significance threshold ($P_{FWER\text{-}corrected} < 0.05$). ***, represents significant p values after correcting for ten multiple comparisons as well as familywise error rate ($P_{FWER\text{-}corrected} < 0.005$). P_T, polygenic score threshold.

Captions

Figure 1. Effect sizes (partial eta squared) of associations between polygenic scores for general intelligence ranging from PS_1 to PS_{10} and *g*-factor performance. All polygenic scores were significantly associated with *g*-factor after Bonferroni correction for ten multiple comparisons (IMAGEN: $F_{1,1640}$= 12.23-94.30; IntegraMooDS: $F_{1,725}$= 9.99-20.98; all $P_{corrected} < 0.05$) except PS_1, which was nominally associated with *g*-factor in IntegraMooDS ($F_{1,725}$= 5.09; $P < 0.05$).

Figure 2. The association of PS_4 ($P_T < 0.001$) and *g*-factor is mediated by cortical thickness in key regions associated with general intelligence in IMAGEN (N = 1,651) and IntegraMooDS (N = 742). Significant vertices are shown ranging from $P_{FWER\text{-}corrected} < 0.005$ (red) to $P_{FWER\text{-}corrected} < 0.001$ (yellow). (**A**) Mediation model statistics from the largest significant cluster (Supplementary Table S7) for associations among PS_4,

cortical thickness and *g*-factor in IMAGEN. Solid arrows represent direct effects, the dotted arrow represents the indirect effect of PS_4 on *g*-factor. (**B**) Brain orientation labels in clockwise direction: rostral, left, superior, inferior, right, caudal. (**C**) Mediation model statistics from the largest significant cluster (Supplementary Table S7) for associations among PS_4, cortical thickness and *g*-factor in IntegraMooDS. Solid arrows represent direct effects, the dotted arrow represents the indirect effect of PS_4 on *g*-factor. (**D**) Brain orientation labels in clockwise direction: rostral, left, superior, inferior, right, caudal.

Figure 3. The association of PS_4 ($P_T < 0.001$) and *g*-factor is mediated by surface area in key regions associated with general intelligence in IMAGEN (N = 1,651) and IntegraMooDS (N = 742). Significant vertices are shown ranging from $P_{FWER\text{-}corrected} < 0.005$ (red) to $P_{FWER\text{-}corrected} < 0.001$ (yellow). (**A**) Mediation model statistics from the largest significant cluster (Supplementary Table S8) for associations among PS_4, surface area and *g*-factor in IMAGEN. Solid arrows represent direct effects, the dotted arrow represents the indirect effect of PS_4 on *g*-factor. (**B**) Brain orientation labels in clockwise direction: rostral, left, superior, inferior, right, caudal. (**C**) Mediation model statistics from the largest significant cluster (Supplementary Table S8) for associations among PS_4, surface area and *g*-factor in IntegraMooDS. Solid arrows represent direct effects, the dotted arrow represents the indirect effect of PS_4 on *g*-factor. (**D**) Brain orientation labels in clockwise direction: rostral, left, superior, inferior, right, caudal.

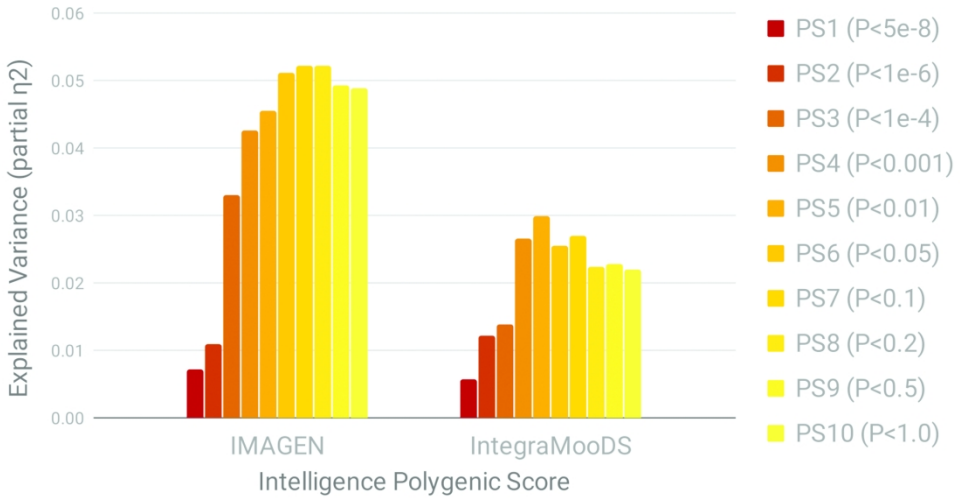

Figure 1

180x93mm (300 x 300 DPI)

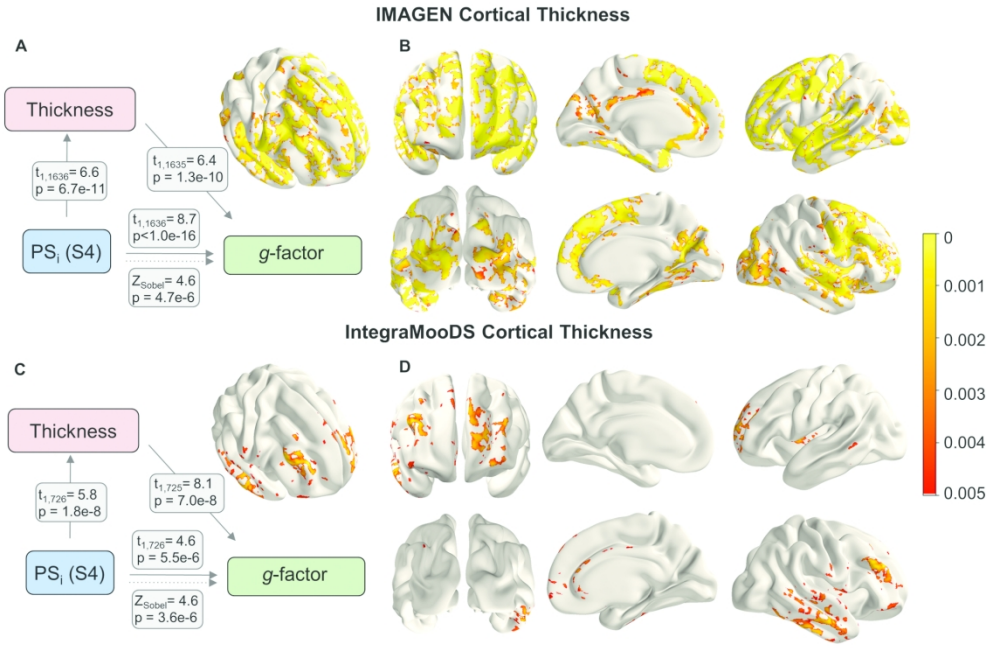

Figure 2

180x119mm (299 x 299 DPI)

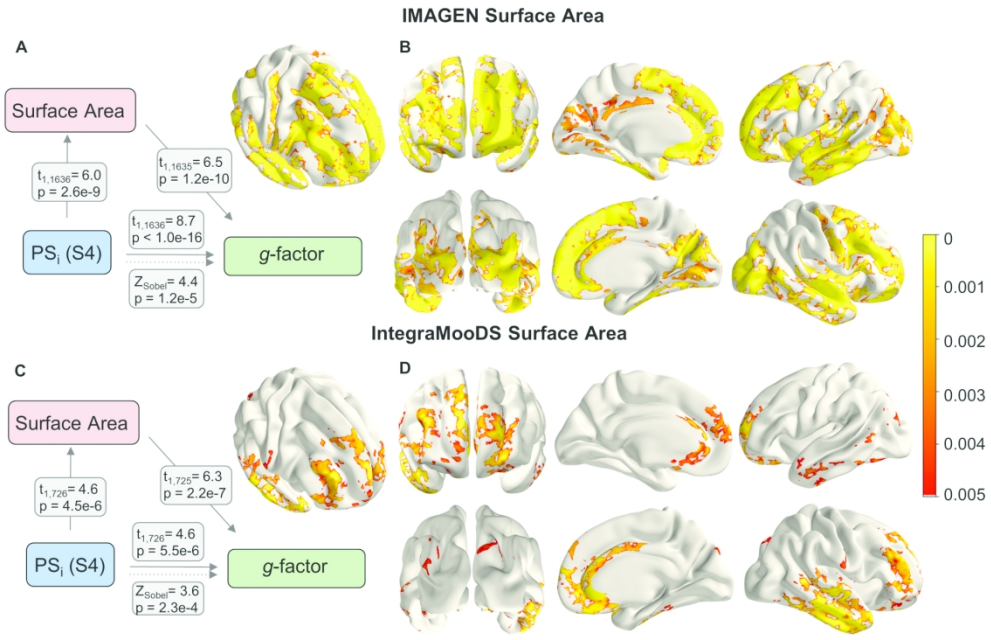

Figure 3

180x118mm (299 x 299 DPI)

Supplementary Material

Cortical surfaces mediate the relationship between polygenic scores for intelligence and general intelligence

Tristram A. Lett[1#*], Bob O. Vogel[1#], Stephan Ripke[1,2,3], Carolin Wackerhagen[1], Susanne Erk[1], Swapnil Awasthi[1,3], Vassily Trubetskoy[1,3], Eva J. Brandl[1], Sebastian Mohnke[1], Ilya M. Veer[1], Markus M. Nöthen[4,5], Marcella Rietschel[6], Franziska Degenhardt[4,5], Nina Romanczuk-Seiferth[1], Stephanie H. Witt[6], Tobias Banaschewski[7], Arun L.W. Bokde[8], Christian Büchel[9], Erin B. Quinlan[10], Sylvane Desrivières[10], Herta Flor[11,12], Vincent Frouin[13], Hugh Garavan[14], Penny Gowland[15], Bernd Ittermann[16], Jean-Luc Martinot[17], Marie-Laure Paillère Martinot[18], Frauke Nees[7,11], Dimitri Papadopoulos Orfanos[13], Tomáš Paus[19], Luise Poustka[20], Juliane H. Fröhner[21], Michael N. Smolka[21], Robert Whelan[22], Gunter Schumann[10] and the IMAGEN consortium, Heike Tost[6], Andreas Meyer-Lindenberg[6], Andreas Heinz[1], Henrik Walter[1*]

Shared first authorship

* Corresponding authors:

Address: Division of Mind and Brain Research, Department of Psychiatry and Psychotherapy CCM, Charité - Universitätsmedizin Berlin; Charitéplatz 1, D-10117 Berlin, Germany.

Email: tristram.lett@charite.de; henrik.walter@charite.de

Telephone: +49 30 450 517 141

Running title: Brain mediators of polygenic score for intelligence

Keywords: Intelligence, Genetics, Mediation, Cortical thickness, Surface area

[1] Department of Psychiatry and Psychotherapy CCM, Charité - Universitätsmedizin Berlin, corporate member of Freie Universität Berlin, Humboldt-Universität zu Berlin, and Berlin Institute of Health, Berlin, Germany
[2] Analytic and Translational Genetics Unit, Massachusetts General Hospital, Boston MA 02114, USA
[3] Stanley Center for Psychiatric Research, Broad Institute of MIT and Harvard, Cambridge MA 02142, USA
[4] Department of Genomics, Life & Brain Center, University of Bonn, Sigmund-Freud-Str. 25, 53127 Bonn, Germany
[5] Institute of Human Genetics, University of Bonn, Sigmund-Freud-Str. 25, 53127 Bonn, Germany
[6] Central Institute of Mental Health, University of Heidelberg, Square J5, 68159 Mannheim, Germany
[7] Department of Child and Adolescent Psychiatry and Psychotherapy, Central Institute of Mental Health, University of Heidelberg, Square J5, 68159 Mannheim, Germany
[8] Discipline of Psychiatry, School of Medicine and Trinity College Institute of Neuroscience, Trinity College Dublin
[9] University Medical Centre Hamburg-Eppendorf, House W34, 3.OG, Martinistr. 52, 20246, Hamburg, Germany
[10] Medical Research Council – Social, Genetic and Developmental Psychiatry Centre, Institute of Psychiatry, Psychology & Neuroscience, King's College London, United Kingdom
[11] Department of Cognitive and Clinical Neuroscience, Central Institute of Mental Health, Medical Faculty Mannheim, University of Heidelberg, Square J5, 68159 Mannheim, Germany
[12] Department of Psychology, School of Social Sciences, University of Mannheim, 68131 Mannheim, Germany
[13] NeuroSpin, CEA, Université Paris-Saclay, F-91191, Gif-sur-Yvette, France
[14] Departments of Psychiatry and Psychology, University of Vermont, 05405 Burlington, Vermont, USA
[15] Sir Peter Mansfield Imaging Centre School of Physics and Astronomy, University of Nottingham, University Park, Nottingham, United Kingdom
[16] Physikalisch-Technische Bundesanstalt (PTB), Abbestr. 2 – 12, Berlin, Germany
[17] Institut National de la Santé et de la Recherche Médicale, INSERM Unit 1000 "Neuroimaging & Psychiatry", University Paris Sud, University Paris Descartes – Sorbonne Paris Cité; and Maison de Solenn, Paris, France
[18] Institut National de la Santé et de la Recherche Médicale, INSERM Unit 1000 "Neuroimaging & Psychiatry", University Paris Sud, University Paris Descartes; Sorbonne Université; and AP-HP, Department of Child and Adolescent Psychiatry, Pitié-Salpêtrière Hospital, Paris, France
[19] Bloorview Research Institute, Holland Bloorview Kids Rehabilitation Hospital and Departments of Psychology and Psychiatry, University of Toronto, Toronto, Ontario, M6A 2E1, Canada
[20] Department of Child and Adolescent Psychiatry and Psychotherapy, University Medical Centre Göttingen, von-Siebold-Str. 5, 37075, Göttingen, Germany
[21] Department of Psychiatry and Neuroimaging Center, Technische Universität Dresden, Dresden, Germany
[22] School of Psychology and Global Brain Health Institute, Trinity College Dublin, Ireland

Intelligence measures

Within IMAGEN, participants completed a battery of neuropsychological tests from the Wechsler Intelligence Scale for Children IV (WISC-IV) (Wechsler 2003). The following subtests were included in

calculating *g*-factor. *Block design* measures the ability of spatial visualization, simultaneous processing, visual-motor coordination and dexterity. Individuals are given coloured blocks and must arrange them to display a printed image. *Similarities* measures abstract reasoning, verbal concept formation and logical thinking. Two related, yet different objects or concepts are presented and participants have to tell how they are alike or different. *Digit Span Forward* and *Digit Span Backward* measure short-term auditory memory and attention. Multiple digits are presented in random order by the examiner. Participants must then recite the digits by recalling them either in the same order (forward) or in reverse order (backward). *Vocabulary* measures verbal fluency, concept formation, word usage, and word knowledge. The examiner either presents a picture or a word is said aloud. Participants are asked to tell the name of the presented object or to define the word. *Matrix reasoning* measures non-verbal problem solving by presenting a matrix of abstract pictures to the participants, where one picture is missing. Participants have to choose the missing picture from multiple options.

In IntegraMooDS, subtests from the Hamburg-Wechsler Adult Intelligence Scale (HAWIE-R) (Wechsler 2008) and other neuropsychological tests were used. The following tests were included for calculating *g*-factor. *Digit Span Forward, Digit Span Backward* and *Matrix reasoning* are identical to the tests used in IMAGEN. *Digit Symbol* measures processing speed, working memory, attention and visuospatial processing. The test consists of a key with the numbers 1-9, each assigned to a unique symbol. Below the key, the numbers 1-9 are randomly listed and participants are asked to write the corresponding symbols, referring to the key, below the numbers in 120 seconds. *Verbal Fluency* as measured by the RWT (Regensburger Wortflüssigkeitstest)(Aschenbrenner et al. 2000), is a test in which participants have to generate as many words as possible, belonging to a category (e.g. fruits, vegetables) in either one or two minutes. *Verbal Intelligence* as measured by the MWT-B (Mehrfachwahl-Wortschatz-Intelligenztest)(Lehrl 1999) is a German instrument measuring crystallized intelligence. The MWT-B consists of 37 multiple-choice items of which only one of five options actually reflects a German word, while the other four are pseudo words. The participants' task is to circle the real words. *Verbal Learning and Memory* as measured by the VLMT (Verbaler Lern- und Merkfähigkeitstest)(Helmstaedter et al. 2001)

is a German instrument measuring different parameters of declarative verbal memory, learning performance, as well as long-term encoding, recall and recognition performance. *Trail Making Test A & B* (Giovagnoli et al. 1996) is a test of visual attention and task switching. In version A, participants have to connect 25 randomly scattered numbers, in the correct order, starting with 1 and ending with 25, without lifting the pen from the paper. In version B, participants have to do the same task and additionally alternate between numbers and letters, (i.e. 1-A-2-B-3-C, etc.). The *D2 Concentration Test (Brickenkamp et al. 1998)* measures selective and sustained attention, as well as visual scanning speed. Participants are required to cross out all letters "d" with two marks surrounding it, with similar surrounding distractor stimuli that do not differ substantially from the target stimulus.

Genetics

In IMAGEN, genotyping was performed using the Illumina Human610Quad chips (Illumina Inc., San Diego, California, USA). In IntegraMooDS genotyping was performed at the Department of Genomics, Life & Brain Center, University of Bonn using the Illumina's Human610Quad, Human660W-Quad and Infinium PsychArray-24 BeadChips. The quality control parameters applied to subjects and SNPs were: SNP missingness < 0.05 (before sample removal); subject missingness < 0.02; autosomal heterozygosity deviation (| Fhet | < 0.2); SNP missingness < 0.02 (after sample removal); difference in SNP missingness between cases and controls < 0.02; and SNP Hardy-Weinberg equilibrium ($P > 10^{-6}$ in controls or $P > 10^{-10}$ in cases). Genotype imputation was performed using the pre-phasing/imputation stepwise approach implemented in EAGLE / MINIMAC3 (with variable chunk size of 132 genomic chunks and default parameters) (Das et al. 2016; "Eagle v2.4.1 User Manual" 2018). The imputation reference set consisted of 54,330 phased haplotypes with 36,678,882 variants from the publically available HRC reference (https://ega-archive.org/datasets/EGAD00001002729). After linkage disequilibrium pruning (r2 > 0.02) and frequency filtering (MAF > 0.05), there were 64,081 autosomal SNPs across both datasets of European ancestry. This SNP set was used for robust relatedness testing and population structure analysis.

Relatedness testing was done with PLINK; pairs of subjects with > 0.2 were identified and one member of each pair removed at random after preferentially retaining cases over controls. After quality control and imputation, 7,644,814 single-nucleotide polymorphisms (SNPs) remained in the IMAGEN sample and 8,843,142 SNPs remained in IntegraMooDS.

We used the standard PGC method for creating polygenic scores across 10 deciles (Ripke et al. 2014). We filtered out variants with an effect allele frequency < 2% and > 98% in the haplotype reference consortium. Variants with less than 80% minimum imputation quality score were excluded. Next, we performed linkage disequilibrium (LD) pruning and clumped the summary statistics, removing variants within 500 kb and $R^2 \geq 0.1$ with, another (more significant) marker. After clumping we had 310,534 LD-independent SNPs available for IMAGEN and 286,154 LD-independent SNPs for IntegraMooDS. For both samples, we calculated PS_i by multiplying the beta estimate of each variant by the imputation probability for the effect allele for each individual. PS_i ranged from S1 to S10 corresponding to p-value thresholds (P_T) from the Savage et al. GWAS (Savage et al. 2018) of: PS_1 ($P_T<5\times10^{-8}$), PS_2($P_T<1\times10^{-6}$), PS_3 ($P_T<1\times10^{-4}$), PS_4 ($P_T<0.001$), PS_5 ($P_T<0.01$), PS_6 ($P_T<0.05$), PS_7 ($P_T<0.1$), PS_8 ($P_T<0.2$), PS_9 ($P_T<0.5$), and PS_{10} ($P_T<=1.0$).

Population stratification principal component estimation was performed with the same collection of autosomal SNPs (IMAGEN: Figure S3; IntegraMooDS: Figure S4). We tested the first four principal components for phenotype association (using logistic regression with study indicator variables included as covariates) and evaluated their impact on the genome-wide test statistics using λ. IMAGEN was separately imputed so was not included in the GWAS meta-analysis thus there was not relatedness testing between all three datasets.

Image acquisition

In IMAGEN, scans were acquired from 3-Tesla scanners from different manufacturers (Siemens, Munich, Germany; Philips, Best, The Netherlands; General Electrics, Chalfont St Giles, UK; Bruker, Ettlingen,

Germany) at eight different sites (King's College, London; Sir Peter Mansfield Imaging Centre of the University of Nottingham; Trinity College Institute of Neuroscience, Dublin; the Centre de Neuroimagerie de Recherche, Paris; Charité Universitätsmedizin Berlin; Universitätsklinikum Hamburg-Eppendorf; Zentralinstitut für seelische Gesundheit, Mannheim; and the Universitätsklinikum Carl Gustav Carus, Dresden). High-resolution anatomical MRIs were acquired, including a three-dimensional (T1-weighted) magnetization prepared gradient echo sequence (MPRAGE) based on the ADNI protocol (for further details see, Schumann et al. 2010).

In IntegraMooDS, structural scans were acquired using T1-weighted three-dimensional magnetization prepared rapid gradient echo (MP-RAGE) sequence with an isotropic spatial resolution of 1 mm^3 (repetition time (TR) = 1.57 s, echo time (TE) = 2.74 ms, flip angle = 15°). Quality control measurements were conducted at all three study sites (Berlin, Bonn, Mannheim) utilizing a multicenter quality assurance protocol (Friedman and Glover 2006), which revealed stable signals over time and comparable quality between sites. Additionally, we included site as a covariate for all statistical analyses.

Processing of structural images

Cortical reconstruction was performed on all T1-weighted images using the Freesurfer image analysis suite (http://surfer.nmr.mgh.harvard.edu/). The technical details of these procedures are described in prior publications (Fischl, Sereno, and Dale 1999; Fischl, Sereno, Tootell, et al. 1999; Fischl and Dale 2000; Fischl et al. 2001, 2004). In brief, this process includes motion correction and averaging of multiple volumetric T1 weighted images, removal of non-brain tissue, automated Talairach transformation, segmentation of the subcortical white matter and deep gray matter volumetric structures, intensity normalization, tessellation of the gray matter white matter boundary, automated topology correction, and surface deformation. A number of deformable procedures were performed including surface inflation, registration to a spherical atlas which is based on individual cortical folding patterns to match cortical geometry across subjects, and creation of a variety of surface based data including maps of curvature and sulcal depth. Both intensity and continuity information from the entire three dimensional MR volume in

segmentation and deformation procedures to produce representations of cortical thickness, calculated as the closest distance from the gray/white boundary to the gray/CSF boundary at each vertex on the tessellated surface (Fischl and Dale 2000). For our analyses, a template of all subjects is created using TFCE_mediation (Lett et al. 2017) employing standard Freesurfer methods. A list of subjects is submitted to create a template with an option for either cortical thickness or surface area. For each subject, surface data is then resampled to the 'fsaverage' using surface-based registration where the cortical manifold is inflated to a sphere and homologous neuroanatomical features are matched (Fischl, Sereno, and Dale 1999; Fischl, Sereno, Tootell, et al. 1999). After registration, all subjects are merged into a single image separately for each hemisphere. The images are smoothed using full-width half maximum (FWHM) of 3mm.

Cortex-wise mediation analysis

TFCE_mediation performs cortex-wise mediation analysis with threshold-free cluster enhancement (TFCE). For a detailed description, please see the methods paper by Lett et al. 2017. In summary, mediation models can be employed to identify the nature of the relationship between an independent variable and two dependent variables (Baron and Kenny 1986). Mediation models assess the relationship between an independent variable and a dependent variable via a mediator (intermediate) variable. The effect of the independent variable on the dependent variable that is explained by a mediator variable is called the indirect effect. TFCE_mediation applies a mediation model at all vertices of a 4D image which then undergo TFCE and significance testing of the indirect effect is assessed via permutation testing. In this study, the mediation analysis was performed with polygenic scores for general intelligence served as the independent variable, cortex-wise images were the mediator variable, and *g*-factor performance scores were the dependent variable. In TFCE_mediation, two sets of regression are performed to assess the indirect effect using the Aroian variant of the Sobel equation (Sobel 1982, 1986; Mackinnon et al. 1995). Significant mediation is assessed using the maximum TFCE transformed z-value from 10,000 permutations. TFCE transformed Sobel z-values that were greater than 95% of the maximum TFCE transformed z-values are deemed significant (i.e., $P_{FWE\text{-}corrected} < 0.05$).

As described in Lett et al. (2017), in TFCE_mediation, sets of regression analyses are performed to assess the indirect (mediation) effect using the Aroian variant of the Sobel equation (Mackinnon et al. 1995; Sobel 1982; Sobel 1986):

$$Z\ value = \frac{a \times b}{\sqrt{b^2 \times S_a^2 + a^2 \times S_b^2 + S_a^2 \times S_b^2}}$$

For Path A, the independent variable (PS_i) is regressed on the mediator variable (brain structure). For Path B, the mediator variable (brain structure) is regressed on the dependent variable (*g*-factor) including the independent variable (PS_i) as a covariate. The unstandardized regression coefficients (betas: a and b) and the standard errors (S_a and S_b) are used to produce a z-value at each vertex of the cortical surface. The z-value then undergoes vertex-wise TFCE transformation, and significance is determined using permutation testing. For additional information please see our methods paper as well as recent publications using TFCE_mediation (Lett et al. 2017; Vogel et al. 2018; Lett et al. 2018). Moreover, the source code and further information are available on the website: https://github.com/trislett/TFCE_mediation.

Online Vertex-wise Results

The association of PS_i ranging from S1 to S10 on vertex-wise measures of cortical thickness and surface area for different $P_{FWER\text{-}corrected}$ thresholds. $P_{FWER\text{-}corrected} < 0.05$ represents the family-wise error rate corrected threshold, $P_{FWER\text{-}corrected} < 0.005$ represents the family-wise error rate as well as Bonferroni corrected threshold for ten multiple comparisons (ten PS_i thresholds). IMAGEN (N = 1,651) included sex, age, site and four population stratification principal components as covariates. IntegraMooDS (N = 742) included subgroup, sex, age, site, and four population stratification principal components as covariates.

Website: https://github.com/bobvogel/g-factor-mediation

Figures and tables

IntegraMooDS	CON	rel-MDD	rel-BPD	rel-SCZ	pat-MDD	pat-BPD	pat-SCZ	Total
Berlin	N = 121	N = 29	N = 21	N = 24	N = 37	N = 32	N = 28	N = 292
Bonn	N = 117	N = 40	N = 33	N = 20	N = 0	N = 0	N = 0	N = 210
Mannheim	N = 101	N = 22	N = 15	N = 23	N = 30	N = 27	N = 22	N = 240
Sex (m/f)	165/174	61/30	41/28	41/26	23/44	27/33	34/16	401/341
Age (M±SD)	33.4±10.3	28.0±9.4	32.6±12.0	32.9±12.7	38.8±13.2	36.5±10.8	33.6±9.0	33.7±11.1
GSI* (M±SD)	0.17±0.17	0.23±0.23	0.20±0.22	0.28±0.35	0.94±0.58	0.97±0.53	0.68±0.48	0.34±0.41
PST* (M±SD)	12.6±11.0	15.7±12.3	14.0±12.5	17.3±16.3	45.5±17.6	35.7±18.1	37.6±21.1	20.1±18.1
PSDI** (M±SD)	1.12±0.36	1.12±0.28	1.13±0.31	1.31±0.54	1.73±0.37	1.5±0.48	1.52±0.39	1.3±0.44

Table S1. Demographic characteristics of the IntegraMooDS sample. * data not available for N=14, ** data not available for N=18. f, female; GSI, symptom checklist 90 global severity index; m, male; M, mean; PSDI, symptom checklist 90 positive symptom distress index; PST, symptom checklist 90 positive symptom total; pat-BPD, patients with bipolar disorder; pat-UPD, patients with unipolar depression; pat-SCZ, patients with schizophrenia; rel-BPD, relatives of patients with bipolar disorder; rel-UPD, relatives of patients with unipolar depression; rel-SCZ, relatives of patients with schizophrenia; SD, standard deviation.

	pat-MDD	pat-BPD	pat-SCZ	Total
Unmedicated	11	3	2	16
SSRI	19	16	6	41
SMS	1	2	-	3
SNRI	13	2	1	16
NDRI	4	4	-	8
MAO-I	1	1	-	2
NaSSA	8	1	-	9
A-AD	1	1	2	4
TCA	11	-	-	11
FGA	-	1	3	4
SGA	12	29	47	88
Lithium	2	22	1	25
Anticonvulsants	1	14	2	17
Valproic acid	-	8	-	8
Benzodiazepines	1	3	-	4
L-Thyroxine	3	9	-	12
Antihistamines	4	3	-	7

Table S2. Medication information for patient groups in IntegraMooDS. Number of individuals without medication information: pat-UPD = 7, pat-BPD = 2, pat-SCZ = 1. A-AD, atypical antidepressant; AC, anticonvulsants; FGA, first generation antipsychotic; MAO-I, monoamine oxidase inhibitor; NaSSA, noradrenergic and specific serotonergic antidepressant; NDRI, norepinephrine-dopamine reuptake inhibitor; pat-BPD, patients with bipolar disorder; pat-UPD, patients with unipolar depression; pat-SCZ, patients with schizophrenia; SGA, second generation antipsychotic; SMS, serotonin modulator and stimulator; SNRI, selective serotonin norepinephrine reuptake inhibitors; SSRI, selective serotonin reuptake inhibitor.

	IMAGEN		IntegraMooDS	
PC	Eigenvalues	% of variance	Eigenvalues	% of variance
1	3.29	41.06	3.66	40.62
2	1.68	21.04	1.17	13.04
3	1.07	13.35	0.91	10.12

Table S3 Eigenvalues and percentage of variance explained for the first three unrotated principal components from different cognitive batteries, separately for IMAGEN and IntegraMooDS.

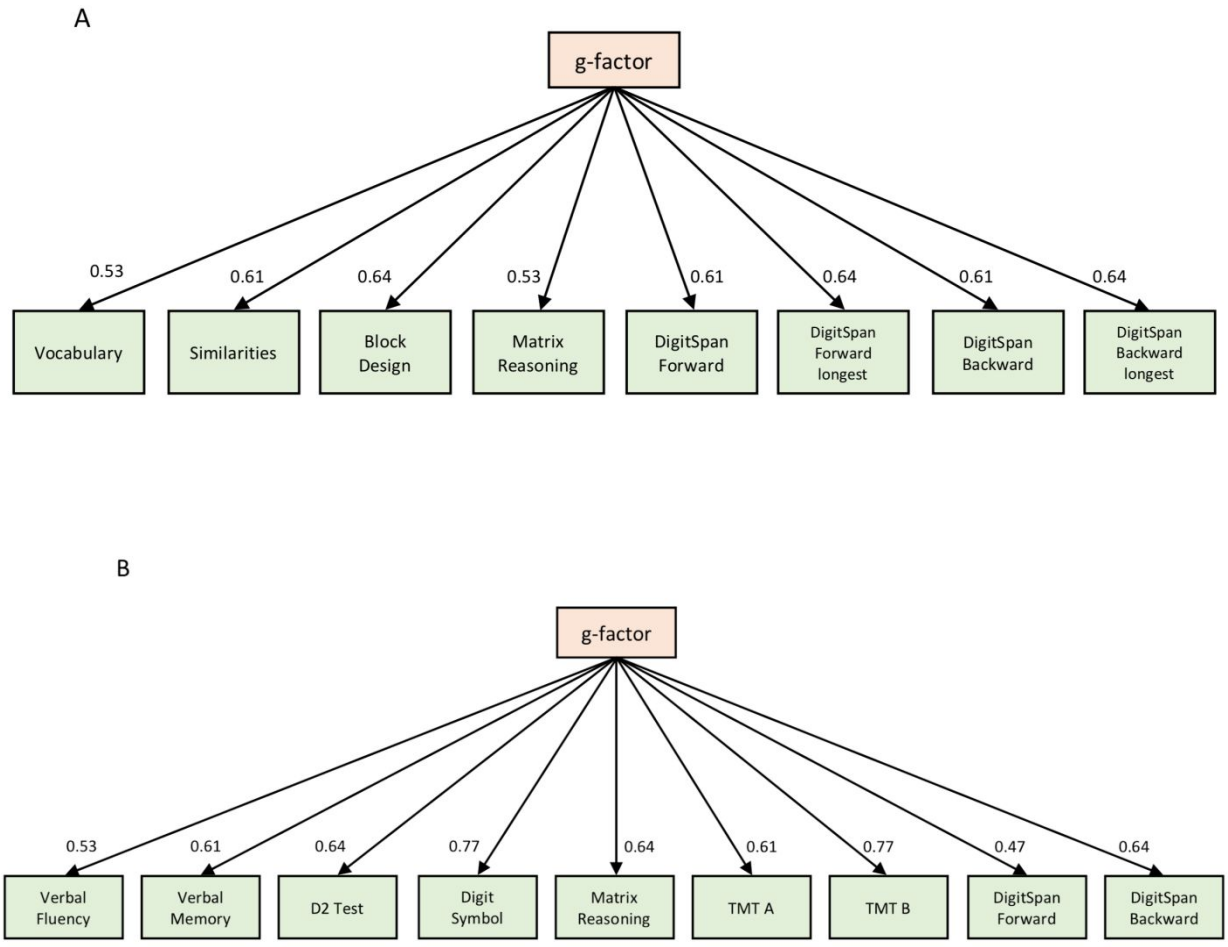

Figure S1. Factor loadings of individual neurocognitive tests on *g*-factor, separately for (**A**) IMAGEN and (**B**) IntegraMooDS. The *g*-factor explained 41.06 % of the variance across the different domains in IMAGEN and 41.72 % in IntegraMooDS.

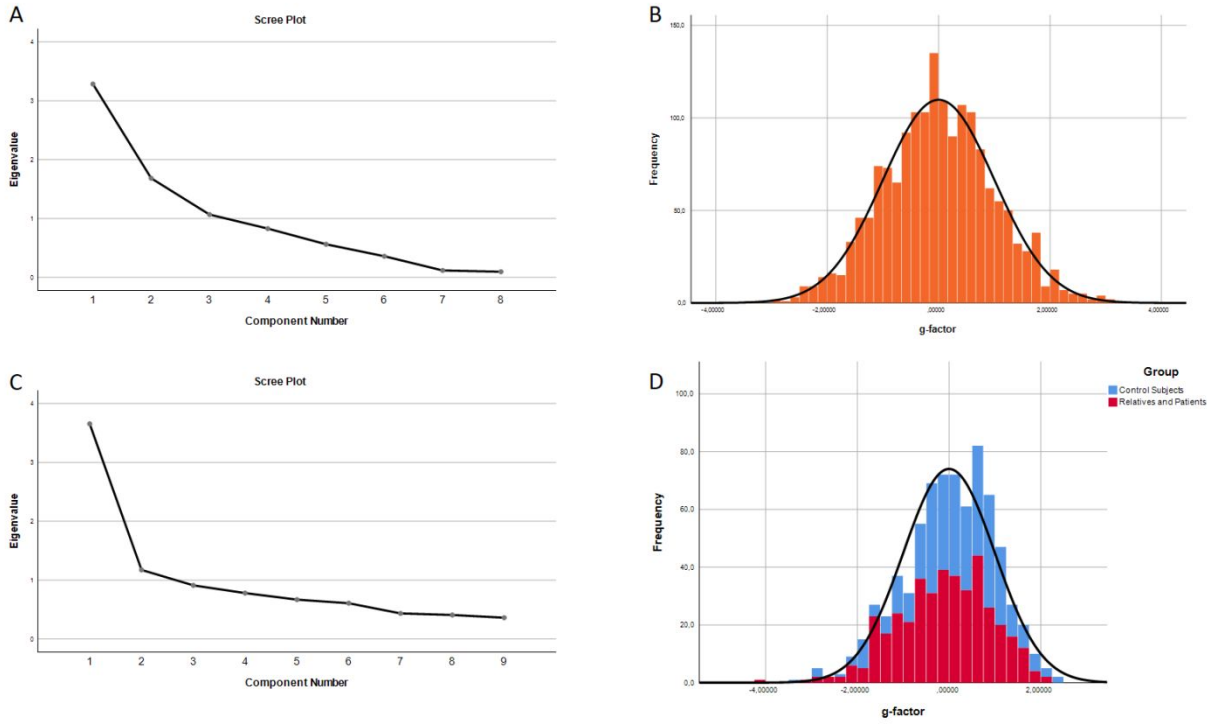

Figure S2 Basic statistics for the principal component analysis. (A) Scree plot for eight principal components from different cognitive batteries in IMAGEN. (B) Histogram for the first unrotated principal component (*g*-factor) in IMAGEN. (C) Scree plot for nine principal components from different cognitive batteries in IntegraMooDS. (D) Histogram for the first unrotated principal component (*g*-factor) in IntegraMooDS, separately for control subjects (blue) as well as relatives and patients (red).

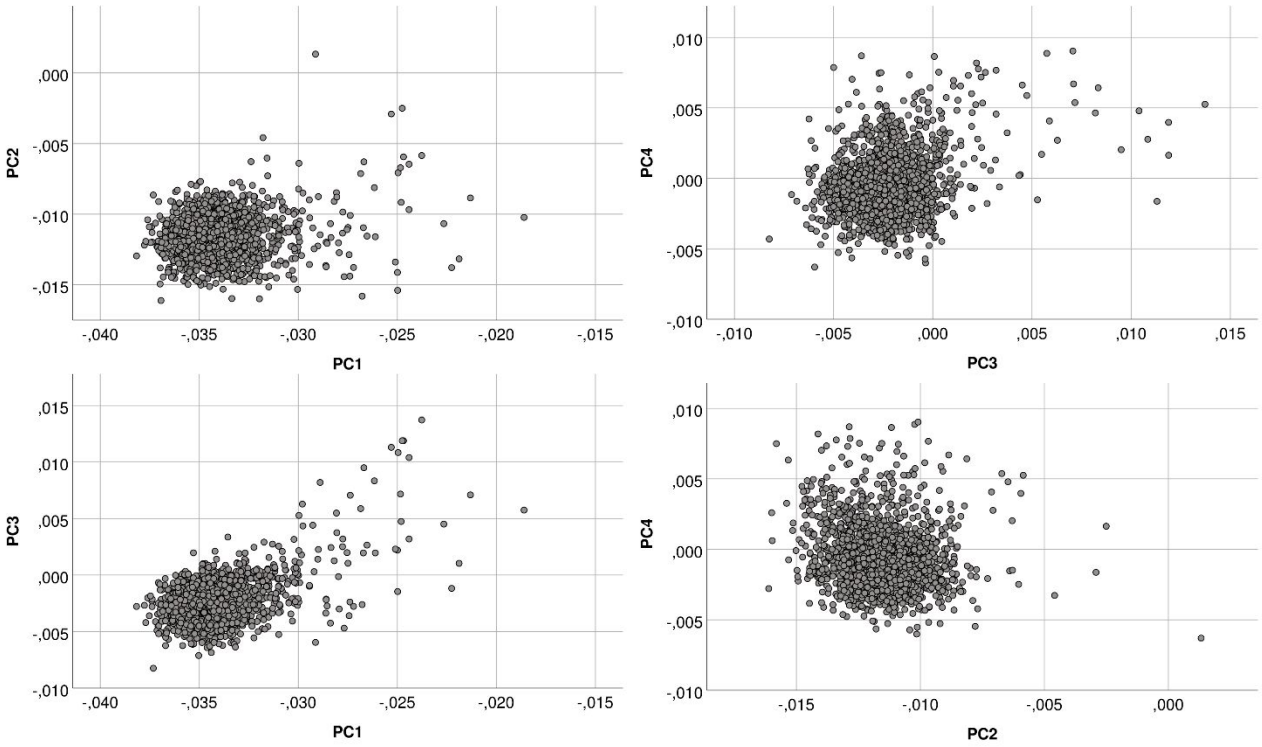

Figure S3. Scatterplots of first four population stratification principal components (PC1 - PC4) in IMAGEN (N=1,651). Population stratification principal component estimation was performed with 64,081 autosomal SNPs. Every dot represents one individual. The clustering of cases clearly indicates common genetic ancestry (all participants were self-report as European-Caucasian).

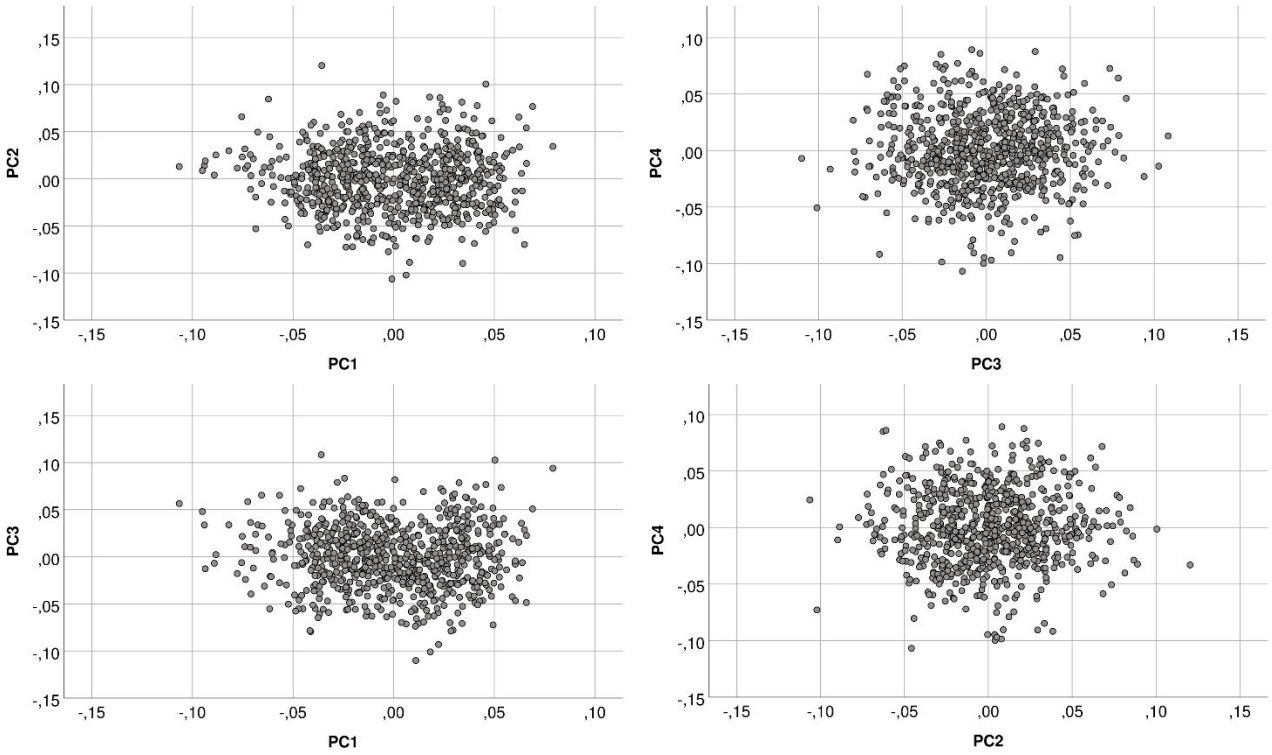

Figure S4. Scatterplots of first four population stratification principal components (PC1 - PC4) in IntegraMooDS (N=742). Population stratification principal component estimation was performed with 64,081 autosomal SNPs. Every dot represents one individual. The clustering of cases clearly indicates common genetic ancestry (all participants were self-report as European-Caucasian).

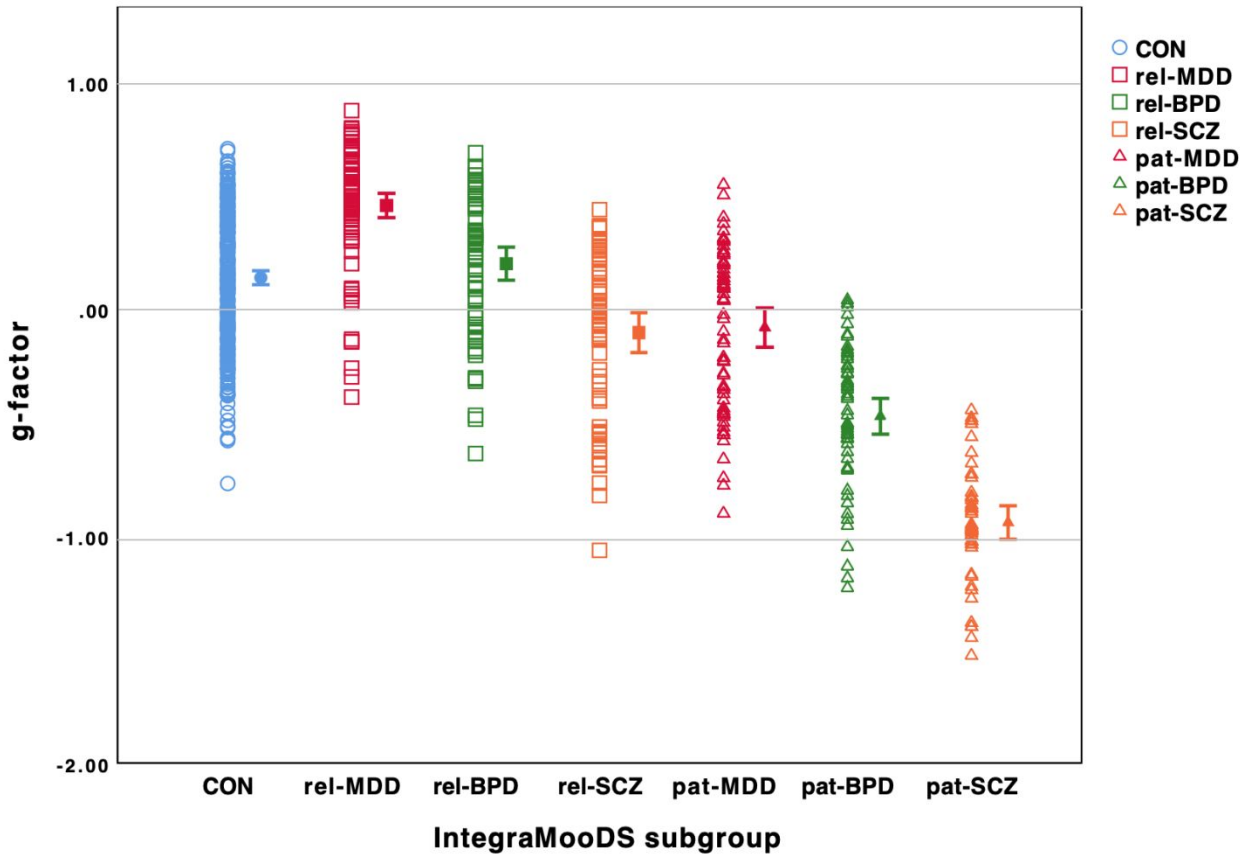

Figure S5. In IntegraMooDS, *g*-factor was significantly different between subgroups after covarying for sex, age, site, and four population stratification principal components ($F_{6,726}$= 9.34, P < 0.001). *g*-factor was significantly lower in schizophrenia relatives (rel-SCZ), patients with bipolar disorder (pat-BPD) and patients with schizophrenia (pat-SCZ) compared to healthy controls, with the greatest difference in pat-SCZ compared to control subjects. Hollow circles, squares and triangles represent each subject of healthy controls, relatives and patients respectively. Mean and 95% confidence interval are shown to the right of each group. For pairwise comparisons see Table S8.

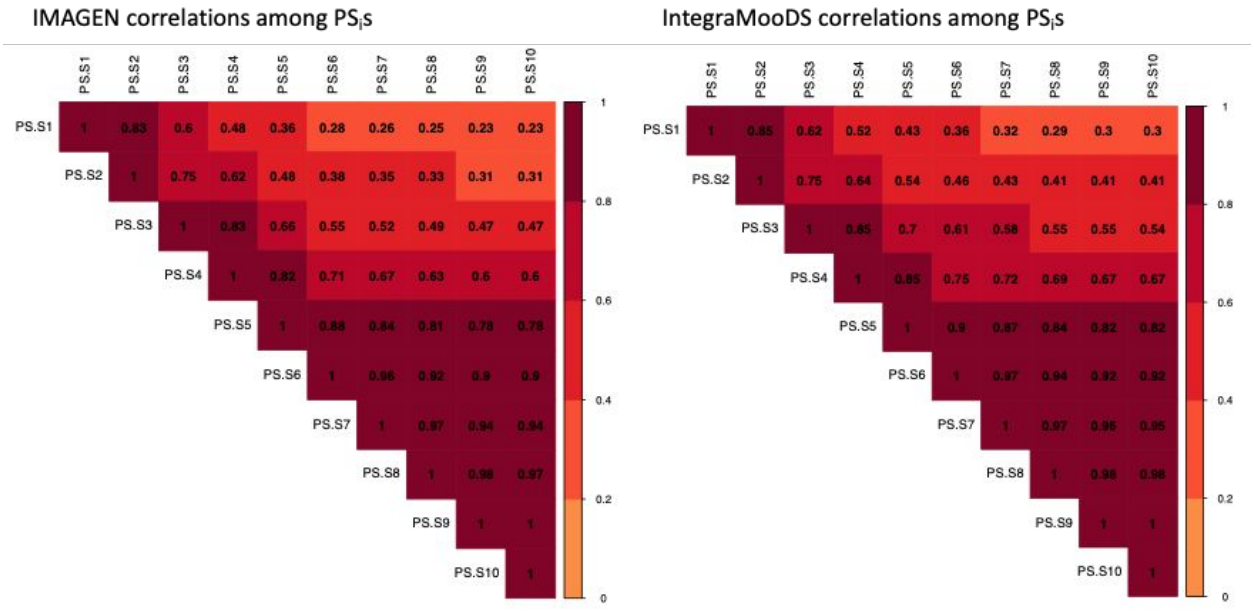

Figure S6. Full correlations between PS_1 to PS_{10} in IMAGEN (left) and IntegraMooDS (right). All correlations were significant after correcting for ten multiple comparisons (all $P_{corrected} < 0.05$). Medium to large correlation coefficients ($r > 0.6$) are observed between PS_4 to PS_{10}.

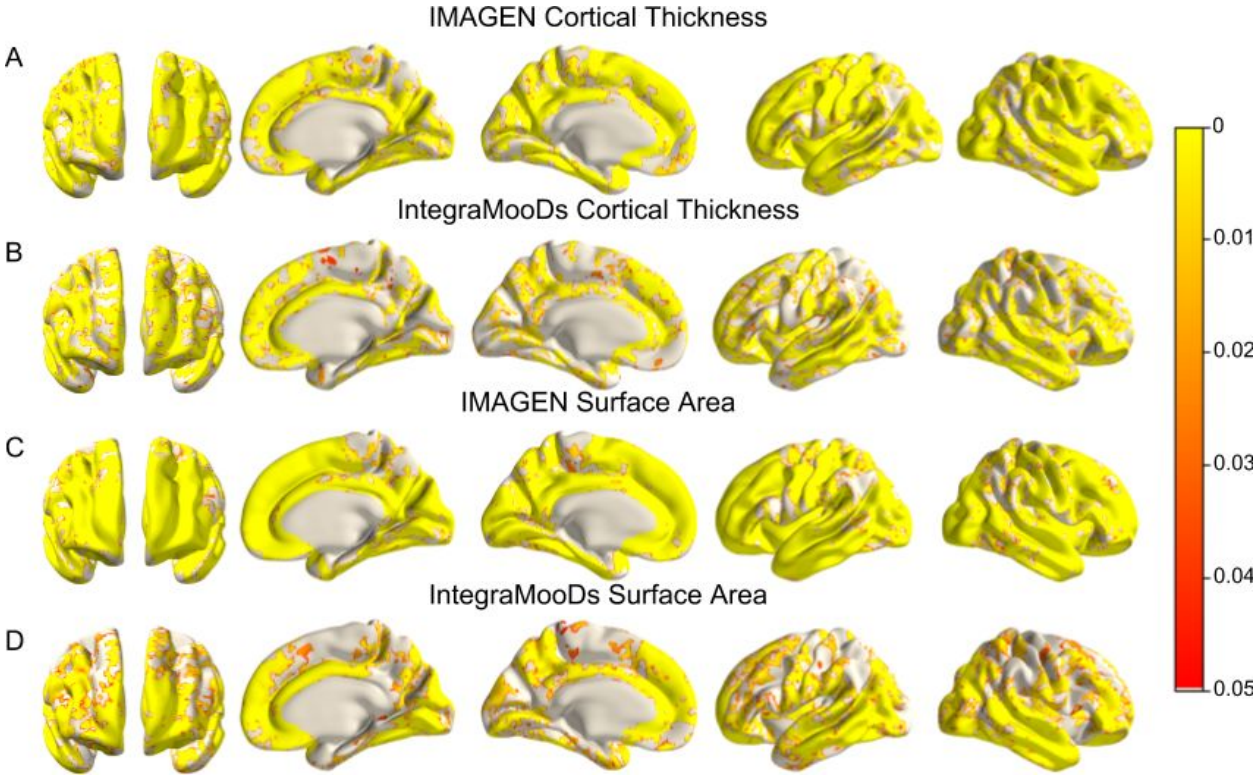

Figure S7. The association of *g*-factor with CT, as well as *g*-factor with SA throughout the cortex ranging from $P_{FWE\text{-}corrected} < 0.05$ (red) to $P_{FWE\text{-}corrected} < 0.001$ (yellow). Anatomical locations from left to right: rostral, left, superior, caudal, right, inferior. IMAGEN included sex, age, site and ethnicity as covariates. IntegraMooDS included subgroup, sex, age, site, and ethnicity as covariates. (**A**) The association of *g*-factor and CT in IMAGEN (N = 1651). (**B**) The association of *g*-factor and CT in IntegraMooDS (N=742). (**C**) The association of *g*-factor and SA in IMAGEN. (**D**) The association of *g*-factor and SA in IntegraMooDS. CT, cortical thickness; SA, surface area.

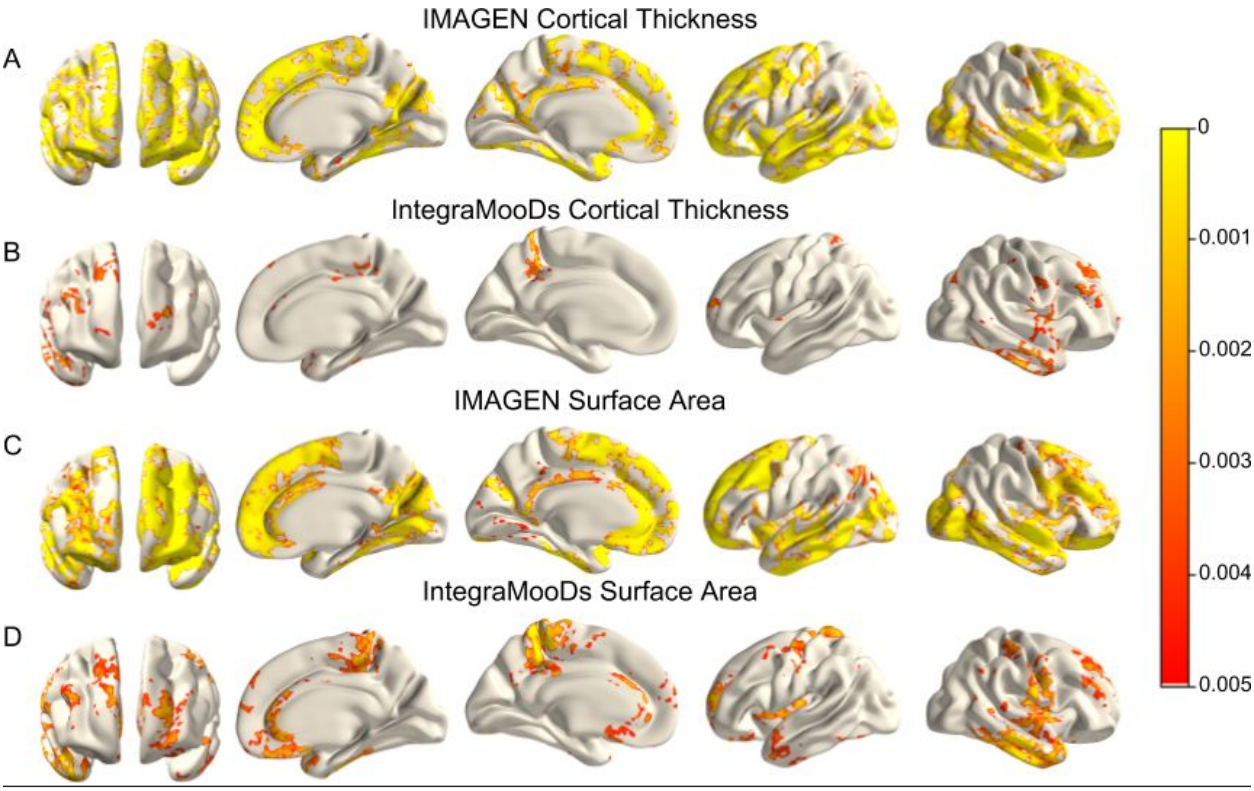

Figure S8. The association of PS_4 with CT, as well as PS_4 with SA in key areas associated with general intelligence differences ranging from $P_{FWE\text{-}corrected} < 0.005$ (red) to $P_{FWE\text{-}corrected} < 0.001$ (yellow). Anatomical locations from left to right: anterior, right inner, left inner, left outer, right outer. IMAGEN included sex, age, site and ethnicity as covariates. IntegraMooDS included subgroup, sex, age, site, and ethnicity as covariates. (**A**) The association of PS_4 and CT in IMAGEN (N = 1651). (**B**) The association of PS_4 and CT in IntegraMooDS (N=742). (**C**) The association of PS_4 and SA in IMAGEN. (**D**) The association of PS_4 and SA in IntegraMooDS. CT, cortical thickness; SA, surface area.

References

Aschenbrenner S, Tucha O, Lange KW. 2000. RWT: Regensburger Wortflüssigkeits-Test. Hogrefe.
Baron RM, Kenny DA. 1986. The moderator--mediator variable distinction in social psychological research: Conceptual, strategic, and statistical considerations. J Pers Soc Psychol. 51:1173.
Brickenkamp R, Zillmer E, Others. 1998. The d2 test of attention. Hogrefe & Huber Seattle, WA.
Das S, Forer L, Schönherr S, Sidore C, Locke AE, Kwong A, Vrieze SI, Chew EY, Levy S, McGue M, Schlessinger D, Stambolian D, Loh P-R, Iacono WG, Swaroop A, Scott LJ, Cucca F, Kronenberg F, Boehnke M, Abecasis GR, Fuchsberger C. 2016. Next-generation genotype imputation service and methods. Nat Genet. 48:1284–1287.
Eagle v2.4.1 User Manual [WWW Document]. 2018. . URL https://data.broadinstitute.org/alkesgroup/Eagle/
Fischl B, Dale AM. 2000. Measuring the thickness of the human cerebral cortex from magnetic resonance images. Proc Natl Acad Sci U S A. 97:11050–11055.
Fischl B, Liu A, Dale AM. 2001. Automated manifold surgery: constructing geometrically accurate and topologically correct models of the human cerebral cortex. IEEE Trans Med Imaging. 20:70–80.
Fischl B, Salat DH, van der Kouwe AJW, Makris N, Ségonne F, Quinn BT, Dale AM. 2004. Sequence-independent segmentation of magnetic resonance images. Neuroimage. 23 Suppl 1:S69–S84.
Fischl B, Sereno MI, Dale AM. 1999. Cortical surface-based analysis. II: Inflation, flattening, and a surface-based coordinate system. Neuroimage. 9:195–207.
Fischl B, Sereno MI, Tootell RBH, Dale AM. 1999. High-resolution intersubject averaging and a coordinate system for the cortical surface. Hum Brain Mapp. 8:272–284.
Friedman L, Glover GH. 2006. Report on a multicenter fMRI quality assurance protocol. J Magn Reson Imaging. 23:827–839.
Giovagnoli AR, Del Pesce M, Mascheroni S, Simoncelli M, Laiacona M, Capitani E. 1996. Trail making test: normative values from 287 normal adult controls. Ital J Neurol Sci. 17:305–309.
Helmstaedter C, Lendt M, Lux S. 2001. Verbaler Lern- und Merkfähigkeitstest: VLMT ; Manual. Beltz-Test.
Lehrl S. 1999. Mehrfachwahl-Wortschatz-Intelligenztest: MWT-B. Spitta.
Lett TA, Waller L, Tost H, Veer IM, Nazeri A, Erk S, Brandl EJ, Charlet K, Beck A, Vollstädt-Klein S, Jorde A, Kiefer F, Heinz A, Meyer-Lindenberg A, Chakravarty MM, Walter H. 2017. Cortical surface-based threshold-free cluster enhancement and cortexwise mediation. Hum Brain Mapp. 38:2795–2807.
Mackinnon DP, Warsi G, Dwyer JH. 1995. A Simulation Study of Mediated Effect Measures. Multivariate Behav Res. 30:41.
Ripke S, Neale BM, Corvin A, Walters JTR, Farh K-H, Holmans PA, Lee. 2014. Biological insights from 108 schizophrenia-associated genetic loci. Nature. 511:421.
Savage JE, Jansen PR, Stringer S, Watanabe K, Bryois J, de Leeuw CA. 2018. Genome-wide association meta-analysis in 269,867 individuals identifies new genetic and functional links to intelligence. Nat Genet. 50:912–919.
Schumann G, Loth E, Banaschewski T, Barbot A, Barker G, Büchel C, Conrod PJ, Dalley JW, Flor H, Gallinat J, Garavan H, Heinz A, Itterman B, Lathrop M, Mallik C, Mann K, Martinot J-L, Paus T, Poline J-B, Robbins TW, Rietschel M, Reed L, Smolka M, Spanagel R, Speiser C, Stephens DN, Ströhle A, Struve M, IMAGEN consortium. 2010. The IMAGEN study: reinforcement-related behaviour in normal brain function and psychopathology. Mol Psychiatry. 15:1128–1139.
Sobel ME. 1982. Asymptotic Confidence Intervals for Indirect Effects in Structural Equation Models. Sociol Methodol. 13:290–312.
Sobel ME. 1986. Some New Results on Indirect Effects and Their Standard Errors in Covariance Structure Models. Sociol Methodol. 16:159–186.
Wechsler D. 2003. Wechsler intelligence scale for children--Fourth Edition (WISC-IV). San Antonio, TX: The Psychological Corporation.
Wechsler D. 2008. WAIS-IV Administration and Scoring Manual. PsychCorp.

Supplementary Table S3 Pairwise comparisons of IntegraMooDS subgroups on *g*-factor perfo
BPD, patients with bipolar disorder; pat-MDD, patients with major depression; pat-SCZ, patient
major depression patients; rel-BPD, relatives of bipolar patients; rel-SCZ, relatives of schizophr

IntegraMooDS subgroups		Mean Difference	Std. Error	Significance (P=0.05)
CON	pat-BPD	0.396	0.155	0.011
	pat-MDD	-0.07	0.15	0.644
	pat-SCZ	0.942	0.163	< 0.001
	rel-BPD	0.016	0.118	0.892
	rel-MDD	-0.147	0.107	0.172
	rel-SCZ	0.284	0.12	0.018
pat-BPD	CON	-0.396	0.155	0.011
	pat-MDD	-0.466	0.156	0.003
	pat-SCZ	0.545	0.169	0.001
	rel-BPD	-0.38	0.195	0.051
	rel-MDD	-0.543	0.19	0.004
	rel-SCZ	-0.112	0.196	0.568
pat-MDD	CON	0.07	0.15	0.644
	pat-BPD	0.466	0.156	0.003
	pat-SCZ	1.011	0.166	< 0.001
	rel-BPD	0.086	0.191	0.655
	rel-MDD	-0.077	0.187	0.679
	rel-SCZ	0.354	0.193	0.067
pat-SCZ	CON	-0.942	0.163	< 0.001
	pat-BPD	-0.545	0.169	0.001
	pat-MDD	-1.011	0.166	< 0.001
	rel-BPD	-0.926	0.2	< 0.001
	rel-MDD	-1.088	0.195	< 0.001
	rel-SCZ	-0.657	0.202	0.001
rel-BPD	CON	-0.016	0.118	0.892
	pat-BPD	0.38	0.195	0.051
	pat-MDD	-0.086	0.191	0.655
	pat-SCZ	0.926	0.2	< 0.001
	rel-MDD	-0.163	0.14	0.245
	rel-SCZ	0.268	0.15	0.075
rel-MDD	CON	0.147	0.107	0.172
	pat-BPD	0.543	0.19	0.004
	pat-MDD	0.077	0.187	0.679
	pat-SCZ	1.088	0.195	< 0.001
	rel-BPD	0.163	0.14	0.245
	rel-SCZ	0.431	0.142	0.002
rel-SCZ	CON	-0.284	0.12	0.018
	pat-BPD	0.112	0.196	0.568
	pat-MDD	-0.354	0.193	0.067
	pat-SCZ	0.657	0.202	0.001
	rel-BPD	-0.268	0.15	0.075
	rel-MDD	-0.431	0.142	0.002

Based on estimated marginal means

ormance scores. CON, control subjects; pat-
ts with schizophrenia; rel-MDD, relatives of
renia patients.

95% Confidence Interval for Difference	
Lower Bound	Upper Bound
0.092	0.701
-0.364	0.225
0.622	1.261
-0.215	0.247
-0.358	0.064
0.049	0.519
-0.701	-0.092
-0.773	-0.159
0.214	0.876
-0.762	0.002
-0.916	-0.17
-0.497	0.273
-0.225	0.364
0.159	0.773
0.686	1.336
-0.29	0.461
-0.444	0.289
-0.024	0.732
-1.261	-0.622
-0.876	-0.214
-1.336	-0.686
-1.319	-0.532
-1.471	-0.706
-1.053	-0.261
-0.247	0.215
-0.002	0.762
-0.461	0.29
0.532	1.319
-0.438	0.112
-0.027	0.564
-0.064	0.358
0.17	0.916
-0.289	0.444
0.706	1.471
-0.112	0.438
0.153	0.71
-0.519	-0.049
-0.273	0.497
-0.732	0.024
0.261	1.053
-0.564	0.027
-0.71	-0.153

Supplementary Table S4 Main effects of polygenic scores at all thresholds (S1-S10) on
largest vertex cluster size (mm²) in each hemisphere. Columns F-H show talairach coordi
descriptions of the cortical parcellation atlas by C. Destrieux in Freesurfer for the left and

CORTICAL THICKNESS

IMAGEN

PSi_Threshold	Lowest pFWER (lh_thickness)	Lowest pFWER (rh_thickness)
PS1 (PT < 5×10−8)	0.1245	0.4598
PS2 (PT < 1×10−6)	0.024	0.0129
PS3 (PT < 1×10−4)	< 0.0001	0.0002
PS4 (PT < 0.001)	< 0.0001	< 0.0001
PS5 (PT < 0.01)	0.0007	0.0003
PS6 (PT < 0.05)	0.0124	0.0015
PS7 (PT < 0.1)	0.0082	0.0019
PS8 (PT < 0.2)	0.0144	0.0027
PS9 (PT < 0.5)	0.0125	0.0057
PS10 (PT < 1.0)	0.0124	0.005

IntegraMooDS

PSi_Threshold	Lowest pFWER (lh_thickness)	Lowest pFWER (rh_thickness)
PS1 (PT < 5×10−8)	0.0119	0.005
PS2 (PT < 1×10−6)	0.0143	0.0016
PS3 (PT < 1×10−4)	0.0086	0.0085
PS4 (PT < 0.001)	0.0006	0.0009
PS5 (PT < 0.01)	0.0036	0.0029
PS6 (PT < 0.05)	0.0322	0.0094
PS7 (PT < 0.1)	0.0222	0.0325
PS8 (PT < 0.2)	0.0182	0.0177
PS9 (PT < 0.5)	0.0104	0.0191
PS10 (PT < 1.0)	0.0097	0.0253

Supplementary Table S5

cortical thickness, separately for IMAGEN and IntegraMooDS. Lowest pFWER indicate the lowest corrected p-valu
nates of the lowest corrected p-value in the left hemisphere and columns I-K show talairach coordinates of the low
right hemisphere. HCP_MMP refers to the the label descriptions of the Glasser 2016 cortical parcellation atlas for

Largest cluster size (lh_thickness)	Largest cluster size (rh_thickness)	X(lh)	Y(lh)	Z(lh)	X(rh)	Y(rh)
0	0	-42.6	-73.68	5.438	27.7	-60.31
158.448883	359.723846	-48.46	-74.58	9.261	49.3	-0.9
32772.09766	33847.09766	-35.13	-23.35	-22.81	7.738	55.656
41284.16016	41362.79297	-22.08	41.541	24.06	38.66	41.046
7056.427734	13367.11328	-35.13	-23.35	-22.81	13.61	35.155
707.39447	8845.519531	-28.74	0.46	-27.75	9.384	52.535
326.291382	5666.798828	-28.74	0.46	-27.75	11.73	35.895
91.403427	5055.89502	-28.74	0.46	-27.75	9.061	54.716
78.954491	4169.319336	-28.74	0.46	-27.75	17.23	34.758
77.948784	2633.052002	-28.74	0.46	-27.75	17.23	34.758

Largest cluster size (lh_thickness)	Largest cluster size (rh_thickness)	X(lh)	Y(lh)	Z(lh)	X(rh)	Y(rh)
240.988	1025.858	-22.83	58.902	12.143	21.1	23.344
266.065	3504.313	-22.83	58.902	12.143	56.56	-36.57
348.763	500.631	-22.83	58.902	12.143	51.42	-3.86
3273.729	6439.737	-7.709	-44.74	45.396	58.08	-21.47
2360.033	2601.952	-23.25	58.355	12.717	50.91	-4.547
40.152	760.691	-36.22	2.039	0.867	46.94	-21.1
152.072	70.542	-30.27	19.968	-21.91	58.58	-23.17
174.005	283.612	-36.22	2.039	0.867	58.58	-23.17
649.657	306.802	-23.25	58.355	12.717	43.48	-18.86
870.282	237.301	-22.83	58.902	12.143	58.58	-23.17

ue observed in the left and right hemisphere. Largest cluster size refers to the
vest corrected p-value in the right hemisphere. APARC shows the label
the left and right hemisphere.

Z(rh)	APARC(lh)	APARC(rh)	HCP_MMP(lh)	HCP_MMP(rh)
34.695	lateraloccipital	superiorparietal	L_MT_ROI	R_MIP_ROI
-15.2	lateraloccipital	superiortemporal	L_LO3_ROI	R_PI_ROI
-10.34	fusiform	medialorbitofrontal	L_TF_ROI	R_10v_ROI
23.971	rostralmiddlefrontal	rostralmiddlefrontal	L_9-46d_ROI	R_46_ROI
25.781	fusiform	superiorfrontal	L_TF_ROI	R_d32_ROI
-3.011	entorhinal	medialorbitofrontal	L_PeEc_ROI	R_10r_ROI
27.229	entorhinal	superiorfrontal	L_PeEc_ROI	R_d32_ROI
-2.852	entorhinal	medialorbitofrontal	L_PeEc_ROI	R_10r_ROI
-21.72	entorhinal	lateralorbitofrontal	L_PeEc_ROI	R_11l_ROI
-21.72	entorhinal	lateralorbitofrontal	L_PeEc_ROI	R_11l_ROI

Z(rh)	APARC(lh)	APARC(rh)	HCP_MMP(lh)	HCP_MMP(rh)
54.669	rostralmiddlefrontal	superiorfrontal	L_p10p_ROI	R_s6-8_ROI
-6.822	rostralmiddlefrontal	middletemporal	L_p10p_ROI	R_STSvp_ROI
7.716	rostralmiddlefrontal	precentral	L_p10p_ROI	R_43_ROI
-29.79	precuneus	inferiortemporal	L_23c_ROI	R_TE2a_ROI
8.063	rostralmiddlefrontal	precentral	L_9a_ROI	R_43_ROI
-26.59	insula	inferiortemporal	L_MI_ROI	R_TF_ROI
-29.45	lateralorbitofrontal	inferiortemporal	L_47s_ROI	R_TE2a_ROI
-29.45	insula	inferiortemporal	L_MI_ROI	R_TE2a_ROI
-23	rostralmiddlefrontal	inferiortemporal	L_9a_ROI	R_TF_ROI
-29.45	rostralmiddlefrontal	inferiortemporal	L_p10p_ROI	R_TE2a_ROI

Supplementary Table S5 Main effects of polygenic scores at all threshold refers to the largest vertex cluster size (mm²) in each hemisphere. Column APARC shows the label descriptions of the cortical parcellation atlas by C

SURFACE AREA

IMAGEN

PSi_Threshold	Lowest pFWER (lh_area)	Lowest pFWER (rh_area)
PS1 (PT < 5×10−8)	0.087317	0.124625
PS2 (PT < 1×10−6)	0.024505	0.063713
PS3 (PT < 1×10−4)	0.0003	0.0016
PS4 (PT < 0.001)	< 0.0001	< 0.0001
PS5 (PT < 0.01)	0.0002	0.0011
PS6 (PT < 0.05)	0.003401	0.006701
PS7 (PT < 0.1)	0.015703	0.013803
PS8 (PT < 0.2)	0.044909	0.027205
PS9 (PT < 0.5)	0.064313	0.045009
PS10 (PT < 1.0)	0.064713	0.05141

IntegraMooDS

PSi_Threshold	Lowest pFWER (lh_area)	Lowest pFWER (rh_area)
PS1 (PT < 5×10−8)	0.1085	0.06
PS2 (PT < 1×10−6)	0.0361	0.0028
PS3 (PT < 1×10−4)	0.0129	0.0082
PS4 (PT < 0.001)	0.0005	0.0005
PS5 (PT < 0.01)	0.0029	0.0017
PS6 (PT < 0.05)	0.0185	0.0072
PS7 (PT < 0.1)	0.0103	0.0056
PS8 (PT < 0.2)	0.0092	0.0028
PS9 (PT < 0.5)	0.0075	0.0064
PS10 (PT < 1.0)	0.0062	0.0062

ds (S1-S10) on surface area, separately for IMAGEN and IntegraMooDS. Lowest pFWER indica
ns F-H show talairach coordinates of the lowest corrected p-value in the left hemisphere and col
. Destrieux in Freesurfer for the left and right hemisphere. HCP_MMP refers to the the label des

Largest cluster size (lh_area)	Largest cluster size (rh_area)	X(lh)	Y(lh)	Z(lh)	X(rh)
0	0	-45.15	-71.04	7.184	35.3
259.596985	0	-43.85	-71.91	5.978	34.9
30791.18359	10591.37305	-24.95	39.407	31.113	49.7
44395.55078	44227.92188	-22.08	41.541	24.06	53.15
17278.80469	14021.77832	-35.79	23.604	46.279	8.824
1374.788696	1556.432739	-35.31	23.764	46.477	45.89
380.515747	384.821594	-35.31	23.764	46.477	45.89
10.46674	122.534241	-35.31	23.764	46.477	45.89
0	7.319267	-35.31	23.764	46.477	45.89
0	0	-35.31	23.764	46.477	45.89

Largest cluster size (lh_area)	Largest cluster size (rh_area)	X(lh)	Y(lh)	Z(lh)	X(rh)
0	0	-44.77	22.01	35.061	63.64
132.073929	3907.442383	-39.58	-7.78	56.735	58.58
2102.220215	2582.749023	-40.66	-8.05	57.708	7.43
17268.07617	14497.2793	-8.153	-50.76	63.943	62.63
8027.92041	7746.904785	-23.46	58.4	11.981	52.36
366.498871	1909.19397	-16.67	58.136	-13.97	46.94
1242.577148	2827.921631	-18.59	57.955	-12.55	46.94
1804.096069	3358.480469	-17.52	58.28	-13.8	46.94
2299.050049	2804.103271	-23.73	57.775	12.483	58.58
2505.432617	2954.635254	-23.73	57.775	12.483	58.58

ate the lowest corrected p-value observed in the left and right hemisphere. Largest cluster size
lumns I-K show talairach coordinates of the lowest corrected p-value in the right hemisphere.
scriptions of the Glasser 2016 cortical parcellation atlas for the left and right hemisphere.

Y(rh)	Z(rh)	APARC(lh)	APARC(rh)	HCP_MMP(lh)	HCP_MMP(rh)
-76.46	35.566	lateraloccipital	inferiorparietal	L_MT_ROI	R_PGp_ROI
-72.55	40.365	lateraloccipital	inferiorparietal	L_MT_ROI	R_IP1_ROI
3.803	-16.43	rostralmiddlefrontal	superiortemporal	L_9-46d_ROI	R_STGa_ROI
-8.565	-2.756	rostralmiddlefrontal	superiortemporal	L_9-46d_ROI	R_TA2_ROI
48.674	16.117	caudalmiddlefrontal	superiorfrontal	L_8Av_ROI	R_9m_ROI
22.777	31.539	caudalmiddlefrontal	rostralmiddlefrontal	L_8Av_ROI	R_p9-46v_ROI
22.777	31.539	caudalmiddlefrontal	rostralmiddlefrontal	L_8Av_ROI	R_p9-46v_ROI
22.777	31.539	caudalmiddlefrontal	rostralmiddlefrontal	L_8Av_ROI	R_p9-46v_ROI
22.777	31.539	caudalmiddlefrontal	rostralmiddlefrontal	L_8Av_ROI	R_p9-46v_ROI
22.777	31.539	caudalmiddlefrontal	rostralmiddlefrontal	L_8Av_ROI	R_p9-46v_ROI

Y(rh)	Z(rh)	APARC(lh)	APARC(rh)	HCP_MMP(lh)	HCP_MMP(rh)
-8.532	19.532	caudalmiddlefrontal	postcentral	L_8C_ROI	R_1_ROI
-23.17	-29.45	precentral	inferiortemporal	L_6d_ROI	R_TE2a_ROI
40.223	6.515	precentral	rostralanteriorcingulate	L_6d_ROI	R_a24_ROI
-10.52	-20.42	precuneus	middletemporal	L_7Am_ROI	R_TE1a_ROI
-44.46	2.856	rostralmiddlefrontal	bankssts	L_p10p_ROI	R_TPOJ1_ROI
-21.1	-26.59	rostralmiddlefrontal	inferiortemporal	L_10pp_ROI	R_TF_ROI
-21.1	-26.59	rostralmiddlefrontal	inferiortemporal	L_a10p_ROI	R_TF_ROI
-21.1	-26.59	rostralmiddlefrontal	inferiortemporal	L_10pp_ROI	R_TF_ROI
-23.17	-29.45	rostralmiddlefrontal	inferiortemporal	L_p10p_ROI	R_TE2a_ROI
-23.17	-29.45	rostralmiddlefrontal	inferiortemporal	L_p10p_ROI	R_TE2a_ROI

Supplementary Table S6 Mediation effects of polygenic scores at all thresholds (S1-S10 refers to the largest vertex cluster size (mm²) in each hemisphere. Columns F-H show tal label descriptions of the cortical parcellation atlas by C. Destrieux in Freesurfer for the lef

CORTICAL THICKNESS

IMAGEN

PSi_Threshold	Lowest pFWER (lh_thickness)	Lowest pFWER (rh_thickness)
PS1 (PT < 5×10−8)	0.5644	0.459
PS2 (PT < 1×10−6)	0.0461	0.0107
PS3 (PT < 1×10−4)	< 0.0001	0.0006
PS4 (PT < 0.001)	< 0.0001	< 0.0001
PS5 (PT < 0.01)	0.0003	0.0007
PS6 (PT < 0.05)	0.0022	0.0017
PS7 (PT < 0.1)	0.0025	0.0017
PS8 (PT < 0.2)	0.0059	0.0023
PS9 (PT < 0.5)	0.0107	0.0083
PS10 (PT < 1.0)	0.0124	0.0078

IntegraMooDS

PSi_Threshold	Lowest pFWER (lh_thickness)	Lowest pFWER (rh_thickness)
PS1 (PT < 5×10−8)	0.0082	0.004
PS2 (PT < 1×10−6)	0.0072	0.0009
PS3 (PT < 1×10−4)	0.0037	0.0022
PS4 (PT < 0.001)	0.0012	0.0011
PS5 (PT < 0.01)	0.0092	0.004
PS6 (PT < 0.05)	0.0279	0.0121
PS7 (PT < 0.1)	0.0359	0.0207
PS8 (PT < 0.2)	0.0134	0.0108
PS9 (PT < 0.5)	0.0082	0.0092
PS10 (PT < 1.0)	0.0092	0.0087

)) on g-factor via cortical thickness, separately for IMAGEN and IntegraMooDS. Lowest pFWER ir
airach coordinates of the lowest corrected p-value in the left hemisphere and columns I-K show ta
t and right hemisphere. HCP_MMP refers to the the label descriptions of the Glasser 2016 cortica

Largest cluster size (lh_thickness)	Largest cluster size (rh_thickness)	X(lh)	Y(lh)	Z(lh)
0.000	0.000	-47.23	-72.63	8.094
2.443	277.331	-47.31	-0.315	-18.05
19586.467	10023.793	-51.07	-7.171	47.498
37452.512	34711.297	-22.08	41.541	24.06
16852.887	9000.147	-17.32	57.987	-4.413
2893.570	3260.671	-51.82	-32.5	6.447
1902.000	2490.322	-51.82	-32.5	6.447
693.237	2432.367	-35.13	-23.35	-22.81
489.733	1227.487	-51.82	-32.5	6.447
444.188	1084.963	-52.95	-31.28	5.775

Largest cluster size (lh_thickness)	Largest cluster size (rh_thickness)	X(lh)	Y(lh)	Z(lh)
474.875	1601.279	-22.29	59.328	11.594
637.607	4040.270	-22.29	59.328	11.594
2508.011	3056.846	-22.29	59.328	11.594
4382.732	5440.993	-22.29	59.328	11.594
374.873	1242.284	-36.56	48.739	16.789
58.449	142.145	-33.67	5.034	4.854
27.625	55.909	-33.67	5.034	4.854
268.242	323.702	-27.79	57.16	-8.752
832.471	497.897	-28.3	57.385	-9.234
789.227	538.844	-27.79	57.16	-8.752

ndicate the lowest corrected p-value observed in the left and right hemisphere. Largest cluster size alairach coordinates of the lowest corrected p-value in the right hemisphere. APARC shows the al parcellation atlas for the left and right hemisphere.

X(rh)	Y(rh)	Z(rh)	APARC(lh)	APARC(rh)	HCP_MMP(lh)	HCP_MMP(rh)
39.52	-75.11	-14.68	lateraloccipital	lateraloccipital	L_MT_ROI	R_PIT_ROI
49.3	-0.9	-15.2	superiortemporal	superiortemporal	L_PI_ROI	R_PI_ROI
49.3	-0.9	-15.2	precentral	superiortemporal	L_55b_ROI	R_PI_ROI
49.42	-6.394	-11.91	rostralmiddlefrontal	superiortemporal	L_9-46d_ROI	R_TA2_ROI
7.161	36.305	46.135	rostralmiddlefrontal	superiorfrontal	L_p10p_ROI	R_8BM_ROI
47.77	30.886	24.979	superiortemporal	rostralmiddlefrontal	L_PBelt_ROI	R_p9-46v_ROI
47.77	30.886	24.979	superiortemporal	rostralmiddlefrontal	L_PBelt_ROI	R_p9-46v_ROI
6.815	38.817	47.105	fusiform	superiorfrontal	L_TF_ROI	R_8BL_ROI
6.815	38.817	47.105	superiortemporal	superiorfrontal	L_PBelt_ROI	R_8BL_ROI
6.815	38.817	47.105	superiortemporal	superiorfrontal	L_PBelt_ROI	R_8BL_ROI

X(rh)	Y(rh)	Z(rh)	APARC(lh)	APARC(rh)	HCP_MMP(lh)	HCP_MMP(rh)
56.05	-36.88	-6.563	rostralmiddlefrontal	middletemporal	L_p10p_ROI	R_STSvp_ROI
64.08	-28.96	-10.58	rostralmiddlefrontal	middletemporal	L_p10p_ROI	R_TE1m_ROI
34.96	44.047	22.839	rostralmiddlefrontal	rostralmiddlefrontal	L_p10p_ROI	R_9-46d_ROI
46.93	32.964	24.541	rostralmiddlefrontal	rostralmiddlefrontal	L_p10p_ROI	R_p9-46v_ROI
42.79	38.167	24.381	rostralmiddlefrontal	rostralmiddlefrontal	L_9-46d_ROI	R_p9-46v_ROI
43.48	-18.86	-23	insula	inferiortemporal	L_MI_ROI	R_TF_ROI
43.48	-18.86	-23	insula	inferiortemporal	L_MI_ROI	R_TF_ROI
43.48	-18.86	-23	rostralmiddlefrontal	inferiortemporal	L_a10p_ROI	R_TF_ROI
43.48	-18.86	-23	rostralmiddlefrontal	inferiortemporal	L_a10p_ROI	R_TF_ROI
43.48	-18.86	-23	rostralmiddlefrontal	inferiortemporal	L_a10p_ROI	R_TF_ROI

Supplementary Table S7 Mediation effects of polygenic scores at all thresholds (S1-S10) on g-factor via
cluster size refers to the largest vertex cluster size (mm²) in each hemisphere. Columns F-H show talairac
hemisphere. APARC shows the label descriptions of the cortical parcellation atlas by C. Destrieux in Frees

SURFACE AREA

IMAGEN

PSi_Threshold	Lowest pFWER (lh_area)	Lowest pFWER (rh_area)	Largest cluster size (lh_area)
PS1 (PT < 5×10−8)	0.2762	0.3782	0.000
PS2 (PT < 1×10−6)	0.0639	0.0442	0.000
PS3 (PT < 1×10−4)	< 0.0001	0.0005	29264.506
PS4 (PT < 0.001)	< 0.0001	< 0.0001	42660.840
PS5 (PT < 0.01)	< 0.0001	< 0.0001	25425.553
PS6 (PT < 0.05)	0.0022	0.0015	6178.632
PS7 (PT < 0.1)	0.0042	0.0029	4394.775
PS8 (PT < 0.2)	0.0063	0.0042	4211.943
PS9 (PT < 0.5)	0.0064	0.0115	4406.553
PS10 (PT < 1.0)	0.0076	0.0124	2093.090

IntegraMooDS

PSi_Threshold	Lowest pFWER (lh_area)	Lowest pFWER (rh_area)	Largest cluster size (lh_area)
PS1 (PT < 5×10−8)	0.0857	0.0283	0.000
PS2 (PT < 1×10−6)	0.0244	0.0003	114.013
PS3 (PT < 1×10−4)	0.0038	0.0009	3792.878
PS4 (PT < 0.001)	0.0002	< 0.0001	9698.590
PS5 (PT < 0.01)	0.0017	0.0011	5220.473
PS6 (PT < 0.05)	0.0084	0.0081	838.145
PS7 (PT < 0.1)	0.0048	0.007	1751.574
PS8 (PT < 0.2)	0.0037	0.0034	2879.789
PS9 (PT < 0.5)	0.0021	0.0026	3524.820
PS10 (PT < 1.0)	0.0017	0.0022	3635.391

surface area, separately for IMAGEN and IntegraMooDS. Lowest pFWER indicate the lowest corrected
ch coordinates of the lowest corrected p-value in the left hemisphere and columns I-K show talairach coo
esurfer for the left and right hemisphere. HCP_MMP refers to the the label descriptions of the Glasser 20

Largest cluster size (rh_area)	X(lh)	Y(lh)	Z(lh)	X(rh)	Y(rh)	Z(rh)	APARC(lh)
0.000	-46.08	-72.38	7.02	38.56	-81.18	27.618	lateraloccipital
27.779	-29.16	57.073	-9.144	8.929	56.514	6.571	rostralmiddlefrontal
14282.280	-21.81	56.186	-13.19	8.977	57.159	7.132	rostralmiddlefrontal
43615.754	-22.08	41.541	24.06	46.94	-21.1	-26.59	rostralmiddlefrontal
16911.369	-17.32	57.987	-4.413	9.505	48.99	14.757	rostralmiddlefrontal
6341.946	-29.18	56.896	-10.26	46.6	23.724	31.427	rostralmiddlefrontal
4142.961	-29.16	57.073	-9.144	45.89	22.777	31.539	rostralmiddlefrontal
2115.740	-29.16	57.073	-9.144	45.89	22.777	31.539	rostralmiddlefrontal
521.712	-29.62	57.059	-9.723	45.89	22.777	31.539	rostralmiddlefrontal
490.109	-29.62	57.059	-9.723	45.89	22.777	31.539	rostralmiddlefrontal

Largest cluster size (rh_area)	X(lh)	Y(lh)	Z(lh)	X(rh)	Y(rh)	Z(rh)	APARC(lh)
112.021	-23.49	57.734	13.212	65.3	-26.42	-12.8	rostralmiddlefrontal
4509.865	-47.13	-78.54	6.384	62.39	-9.44	-19.97	lateraloccipital
6078.794	-23.49	57.734	13.212	5.605	31.58	-7.035	rostralmiddlefrontal
11148.153	-23.25	58.355	12.717	6.6	35.606	15.767	rostralmiddlefrontal
8333.247	-23.25	58.355	12.717	6.588	37.175	-2.865	rostralmiddlefrontal
1218.548	-17.07	58.289	-14.43	6.588	37.175	-2.865	rostralmiddlefrontal
1738.670	-17.07	58.289	-14.43	58.58	-23.17	-29.45	rostralmiddlefrontal
2786.787	-13.87	57.902	-7.452	6.197	36.335	-3.754	rostralmiddlefrontal
2822.033	-23.73	57.775	12.483	6.602	37	-3.415	rostralmiddlefrontal
2867.298	-23.78	56.992	12.122	6.602	37	-3.415	rostralmiddlefrontal

d p-value observed in the left and right hemisphere. Largest
ordinates of the lowest corrected p-value in the right
016 cortical parcellation atlas for the left and right hemisphere.

APARC(rh)	HCP_MMP(lh)	HCP_MMP(rh)
inferiorparietal	L_MT_ROI	R_PGp_ROI
superiorfrontal	L_a10p_ROI	R_9m_ROI
superiorfrontal	L_11l_ROI	R_9m_ROI
inferiortemporal	L_9-46d_ROI	R_TF_ROI
superiorfrontal	L_p10p_ROI	R_9m_ROI
rostralmiddlefrontal	L_11l_ROI	R_p9-46v_ROI
rostralmiddlefrontal	L_a10p_ROI	R_p9-46v_ROI
rostralmiddlefrontal	L_a10p_ROI	R_p9-46v_ROI
rostralmiddlefrontal	L_11l_ROI	R_p9-46v_ROI
rostralmiddlefrontal	L_11l_ROI	R_p9-46v_ROI

APARC(rh)	HCP_MMP(lh)	HCP_MMP(rh)
middletemporal	L_9a_ROI	R_TE1m_ROI
middletemporal	L_LO3_ROI	R_TE1a_ROI
rostralanteriorcingulate	L_9a_ROI	R_a24_ROI
rostralanteriorcingulate	L_9a_ROI	R_p24_ROI
rostralanteriorcingulate	L_9a_ROI	R_a24_ROI
rostralanteriorcingulate	L_10pp_ROI	R_a24_ROI
inferiortemporal	L_10pp_ROI	R_TE2a_ROI
rostralanteriorcingulate	L_10pp_ROI	R_a24_ROI
rostralanteriorcingulate	L_p10p_ROI	R_a24_ROI
rostralanteriorcingulate	L_p10p_ROI	R_a24_ROI

Supplementary Table S8 *Post hoc* estimation of effect Sizes (partial eta squared; η^2) at all signi
well as the partial mediation effect (Path C').

IMAGEN	Total Effect (Path C)	Path A Cortical Thickness	Path A Surface Area	Path B Cortical Thickness	Path B Surface Area
PS1	0.007341444	N.A.	N.A.	N.A.	N.A.
PS2	0.011288056	0.010637563	0.007128391	0.023009107	0.024495129
PS3	0.034070055	0.015968479	0.013033482	0.03296986	0.030807555
PS4	0.044056335	0.017223893	0.013469027	0.033639848	0.0307803
PS5	0.04695954	0.012664593	0.009577288	0.035199446	0.032196801
PS6	0.052673735	0.010745356	0.00878965	0.033123016	0.028450697
PS7	0.053783554	0.010329098	0.007851592	0.032593943	0.028085812
PS8	0.053856674	0.009052642	0.006288853	0.032647805	0.027802607
PS9	0.05080042	0.009507424	0.005495145	0.030567196	0.026976478
PS10	0.050385935	0.009122938	N.A.	0.028491337	N.A.

IntegraMooDS	Total Effect (Path C)	Path A Cortical Thickness	Path A Surface Area	Path B Cortical Thickness	Path B Surface Area
PS1	N.A.	0.023710459	N.A.	0.007637632	N.A.
PS2	0.01400802	0.033905557	0.022968542	0.026332729	0.022941023
PS3	0.013978679	0.021330956	0.014364423	0.009089858	0.014390761
PS4	0.027986736	0.028084772	0.021597315	0.028414299	0.024332036
PS5	0.028122722	0.019231866	0.021463675	0.009066923	0.018182193
PS6	0.023449613	0.023978284	0.017451837	0.017872337	0.015780719
PS7	0.024505001	0.012148968	0.021441027	0.010886008	0.017097051
PS8	0.020475214	0.024107165	0.021619755	0.015767443	0.016290359
PS9	0.021363345	0.022828202	0.020505194	0.013884041	0.024852741
PS10	0.020631827	0.027669158	0.020491315	0.013532271	0.024842213

ificant PSi thresholds including: the total effect (Path A; PSi on g-factor), Path A (PSi on brain struc

Partial Mediation Effect Cortical Thickness	Partial Mediation Effect Surface Area	Percentage of explainable variance in g-factor explained by mediation Cortical	Percentage of explainable variance in g-factor explained by mediation
N.A.	N.A.	N.A.	N.A.
0.002810384	0.002135464	24.90%	18.92%
0.006652322	0.005801591	19.53%	17.03%
0.007488177	0.006518521	17.00%	14.80%
0.006667483	0.0056281	14.20%	11.98%
0.006331695	0.005195855	12.02%	9.86%
0.006191664	0.004923564	11.51%	9.15%
0.00573453	0.004290712	10.65%	7.97%
0.005639204	0.003859965	11.10%	7.60%
0.005336247	N.A.	10.59%	6.28%

Partial Mediation Effect Cortical Thickness	Partial Mediation Effect Surface Area	Percentage of explainable variance in g-factor explained by mediation Cortical Thickness	Percentage of explainable variance in g-factor explained by mediation Surface Area
0.0018693	N.A.	24.88%	N.A.
0.005740155	0.004521918	40.98%	32.28%
0.002797127	0.002914643	20.01%	20.85%
0.00759893	0.006231006	27.15%	22.26%
0.003439244	0.005414326	12.23%	19.25%
0.005219242	0.004145528	22.26%	17.68%
0.003028545	0.004943961	12.36%	20.18%
0.004629118	0.004340062	22.61%	21.20%
0.004386633	0.005123405	20.53%	23.98%
0.004322695	0.005028373	20.95%	24.37%

cture), Path B (Brain structure on g-factor), as